

Impact of *Spartina alterniflora* invasion on evapotranspiration water loss in *Phragmites australis* dominated coastal wetlands of east China

Taitiya Kenneth Yuguda^a, Yueming Wu^a, Zhanrui Leng^a, Guifeng Gao^c, Guanlin Li^a, Zhicong Dai^a, Jian Li^{a,b,*}, Daolin Du^a

^a Institute of Environment and Ecology, School of Environment and Safety Engineering, Jiangsu University, Zhenjiang 212013, PR China

^b State Key Laboratory of Marine Environmental Science, Xiamen University, Xiamen 361102, PR China

^c State Key Laboratory of Soil and Sustainable Agriculture, Institute of Soil Science, Chinese Academy of Sciences, 71 East Beijing Road, Nanjing 210008, China

ARTICLE INFO

Keywords:

Wetlands
Ecohydrology
Evapotranspiration
Water loss
Biological invasions
Invasive plants
Water resources

ABSTRACT

A comparative analysis of co-existing invasive and native wetland plants is a practical approach to exploring exotic plant invasiveness. *Spartina alterniflora* is an invasive C₄ grass, prevalent in China's coastal wetlands and other parts of the world, posing a risk to the hydrological cycle. While the crop coefficient K_c and evaporative water loss of the invasive *S. alterniflora* are still considerably unexplored, we utilized field measurements and a modeling technique to evaluate water loss to Evapotranspiration ET in marshes with *S. alterniflora* and *P. australis*. Changes in surface resistance, canopy height, and the technique used to calculate net radiation from incoming solar radiation have all been shown to influence the Penman-Monteith methodology for estimating ET. Overall, *S. alterniflora* surpassed *P. australis* in leaf area index LAI, ET, crop coefficient K_c, peak net photosynthetic rate, and growing season. Daily ET values in both plants ranged from 0.98 to 6.35 mm/day and 1.91 to 8.16 mm/day during the monitoring period. According to regression analysis, the key driving factors of ET from both plant communities throughout the growing season are net radiation, soil moisture, relative humidity, air temperature, and surface temperature. These findings highlight the necessity of precisely determining these parameters based on site-specific data instead of depending on empirical models developed mainly for crops and forests. Given the mean ET rates found in this study, *S. alterniflora* invasion in China currently accounts for ~4.3 × 10⁶ m³ day⁻¹ of water loss to ET, posing a severe threat to the availability of water resources in China's wetlands. Our findings contribute to a better understanding of the link between plant invasiveness and water loss in wetlands, offering stakeholders a benchmark for achieving future goals and plans related to the utilization of wetland water resources worldwide.

1. Introduction

Biological invasions are one of the most critical concerns facing today's global environmental change, in which wetlands are viewed as critical components of the ecosystem that play vital roles in sustaining a healthy environment. Owing to increasing biomass and ET of wetland vegetation, ET is a crucial facet of the water budget and energy balance, notably on wetland sites (Yan et al., 2017). It has an effect on the diversity, structure, and restoration of wetland vegetation ecosystems (Zhang et al., 2018). However, due to ET from emergent plants, wetlands experience significant water losses from the open water surface, which consequentially impacts regional water cycling (Pauliukonis and Schneider, 2001). Although invasive alien plant species (IAPs) are

widely recognized as the "most significant direct causes of negative ecological impacts in coastal wetlands habitats," it is also believed that IAPs have a detrimental effect on water resources due to their excessive water demand and usage (ET) in comparison to native plant communities (Meijninger and Jarman, 2014).

Invasive plants are presumed to overwhelmingly exploit more resources than native plants in several ecosystems, contributing to detrimental effects on water resources and the ecohydrology of an ecosystem (Brauman et al., 2007). Compared to native plants, the characteristics that render a plant species invasive can lead to excessive absolute water usage. Fast-growing species are likely to consume more water than subsequent continuous or steady growing species (Irvine et al., 2004) while also evolving more rapidly than their native correlates (Grotkopp

* Corresponding author at: Institute of Environment and Ecology, School of Environment and Safety Engineering, Jiangsu University, Zhenjiang 212013, PR China.
E-mail address: jianli@ujs.edu.cn (J. Li).



et al., 2002). However, “interruptions” often occur when comparing mechanisms for contrasting species water usage at the leaf, stem, and ecosystem expanse (Wullschleger et al., 1998). Invasive plant species cause physical and biological changes in coastal habitats, affecting water quantity and quality. Presently, a significant body of evidence reported IAPS to exacerbate transpiration and evaporation losses, consequently affecting runoff quantity and timing, flooding, sedimentation, and other natural physical processes, as well as water supply in general (Catford, 2017; Dzikiti et al., 2016; Everard, 2020; Le Maitre et al., 2020; McCormick and Contreras, 2009; Meijninger and Jarmain, 2014; Swaffer and Holland, 2015; Tang et al., 2020).

Previous ecohydrology research centered on the ecosystem-scale water productivity of combined wetlands with the distinctive community and water usage in invasive alien plants IAPS dominated systems. Compared to wetland species, many terrestrial species have higher ET rates and a more stable daily flux (Pauliukonis and Schneider, 2001). Differences in study site characteristics values for crop coefficients (K_c) varied widely. It was not considered necessary to combine results to generate a single set of monthly mean values when using the lysimeter technique to determine evapotranspiration (ET) rates in large reed beds (Fermor et al., 2001; Read et al., 2008). With ET rates higher than the Penman Potential Evaporation at both sites, the ET estimates of a reed bed were 15% higher than that of a grassland wetland. The disparities between sites are due to the reed's total surface resistance being lower and its surface roughness length being longer (Acreman et al., 2003). Stands of the invasive reed *A. donax* utilized roughly 8.09 mm/day of water at the peak of the growing period, showing that this rate of water usage is on the extreme end of the scale for plants (Watts and Moore, 2011). Despite the fact that the subsequent growing season was wetter, the seasonal ET of the invasive giant reed *Arundo donax L.* 842 mm was significantly greater than in the succeeding season 625 mm (Racelis et al., 2021).

Improved ET prediction for native *Tamarix ramosissima* is possible thanks to temporal and ecosystem-specific ET trends. The mean daily ET was 1.62 mm/day and a seasonal total of 248.2 mm using Bowen ratio data and calculating seasonal ET and developing an energy balance (Si et al., 2005). In addition to environmental and climatic factors, vegetation's growth condition and biotic factors, particularly the leaf index and leaf conductance, have a major impact on the ET of *Phragmites* populations (Yu et al., 2008a). Employing shallow differences in the water table and the ALMANAC model, the monthly average approximate daily water use rates of invasive Reed canary grass (*Phalaris arundinacea*) were 3.3 mm/d in July and 2.3–2.8 mm/d between May and September (Schilling and Kiniry, 2007). Over a two-year period, annual average ET rates increased by approximately 3 mm/day in response to the growth of the reed (*P. australis*) community. This indicates that ET values were higher in the summer than in the autumn and that they correlate to *P. australis'* maximum standing biomass (Headley et al., 2012). Deploying eddy covariance technique, daily ET rates of *P. australis* ranged from 0.1 mm day⁻¹ to 5.8 mm day⁻¹, accounting for around 13% of annual ET loss (Zhou and Zhou, 2009). Based on the Penman-Monteith formula and water balance approach, cumulative ET for *P. australis* in Italy ranged from 3048 mm to 3899 mm, demonstrating the impact of advection on ET rates (Borin et al., 2011). Whereas in pilot-built wetlands planted with five distinct Perennial Plant species, *P. australis* had the highest overall seasonal mean ET value 17.31 mm d⁻¹ (Milani et al., 2019).

The mean annual ET from lands dominated by IAPs, natural vegetation, alien forest trees, and experimental (control) fields were compared using spatial ET data and GIS-based land-use data. The ET of the five dominant IAPs (895 mm) was much more than that of other native species (Meijninger and Jarmain, 2014). In a southern South American salt marsh dominated by *Spartina densiflora* and *Sarcocornia ambigua*, (Gassmann et al., 2019) used the coupled Penman-Monteith and surface resistance methods to determine that surface resistance can be achieved using a small number of variables that can be calculated

in the field, allowing for the estimation of ET in salt marsh environments with limited meteorological data. Various approaches for measuring ET rates have been established, including lysimeter techniques, Eddy covariance method, and Bowen ratio energy balance (BREB). Lysimeters are still the most effective method for directly measuring ET rates, though managing them takes time and effort (Borin et al., 2011; Hassan et al., 2008). Utilizing the BREB approach, a fault in one instrument significantly affects all determined fluxes; however, when the latent and sensible heat fluxes are about the same in magnitude but in opposing directions, the approach fails (Unland et al., 1996). Equipment in the Eddy Covariance technique does not perform effectively when mist or precipitation falls on it in the morning (Burba et al., 2007; Twine et al., 2000).

Compared to other approaches that use onsite measured meteorological variables; FAO 56 methods, Priestley-Taylor, Turc-Radiation, FAO-Blaney-Criddle, and FAO-Radiation (Zhao et al., 2005), the Penman-Monteith eq. (PM) is currently the most widely used method for calculating ET within various soil moisture factors (Ma et al., 2016; Yuguda et al., 2020). It has been applied in wetlands and found to be in good agreement when validated with other approaches (Drexler et al., 2004; Souch et al., 1998; Souch et al., 1996; Wessel and Rouse, 1994). Carbon assimilation, solar irradiance, air temperature, vapor deficit, near-surface atmospheric turbulence, plant transpiration rate, leaf area index (LAI), and soil moisture all influence the variability of parameters (Gassmann et al., 2019). A rise in surface resistance r_s causes a decrease in ET, resulting in elevated surface temperatures and sensible heat fluxes (Jarvis and McNaughton, 1986), while the Priestly-Taylor (PT) and PM methods performed similarly, with PM yielding better outcomes (Souch et al., 1996).

While the crop coefficient K_c and evaporative water loss of invasive *S. alterniflora* have remained largely unexplored, this is the first study to compare ET of invasive *S. alterniflora* with native *P. australis* in a coastal salt marsh. The aim of this study was thus to deploy field measurements and mathematical models to examine the ET characteristics of an invasive and native wetland plant and explore the long-term viability of coastal wetland reclamation in terms of water loss. Our findings will close an information gap in our understanding of ET water depletion from one of the world's most extensive reclamation coastlines, which would be crucial for the long-term conservation of wetlands water resources.

2. Materials and methods

2.1. Study area

The study area Fig. 1, is in the Liangduo estuary on Jiangsu Province's south-central coast, with geographical coordinates of 120°48' 120°52'E and 33°04' 32°08'N. The yearly mean temperature is 13.7 and 14.8 °C, with 1010 mm precipitation. The region is a conventional coastal lowland characterized by sediment supplies from the estuary of the Yellow River and the Yangtze River, generating an exceptionally long sediment muddy coast and creating wide expanse beach features. The tidal flat is around 5000 km², nearly a quarter of China's land area. It is located in a macrotidal environment, with a mean tidal range of 3.9–5.5 m and a semi-diurnal tide regularly (Chen, 2013). From Sheyang delta to Liangduo delta, the shoreline mean littoral zone and mean rising sea level significantly increase, signifying a sizable tidal area with a wide intertidal zone and speedy momentum. It features a tropical monsoon, abundant rainfall, and coastal marshland vegetation. The region's tidal wetland resources are enormously abundant in biodiversity, and Yancheng's red-crowned crane National Nature Reserve is located in parts of these wetlands. According to the formation mechanism, the soils near the coast are divided into three categories: Anthrosols, Fluvisols, and Cambisols (Fang et al., 2010). From the coast to the inland, the vegetation community is scattered layered. *S. alterniflora* predominate *P. australis* from the coast through bare tidal flats. Because of its

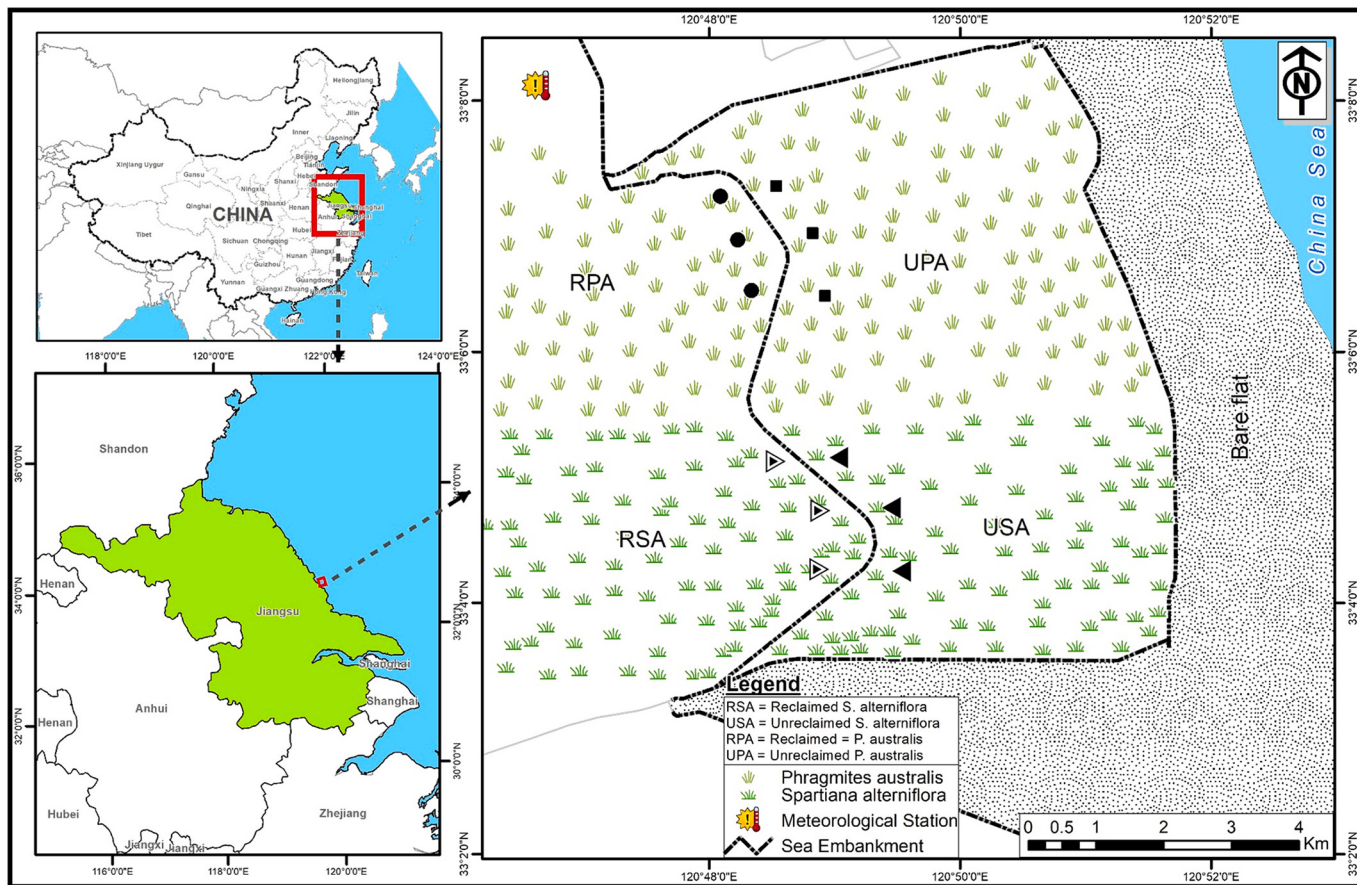


Fig. 1. Study area map showing *S. alterniflora* and *P. australis* communities.

importance in biodiversity conservation, the region has become a hub of wetland study.

2.2. Field experiments

We chose the lysimeter method to measure daily ET rates because it is the most reliable method for applying a uniform procedure over many plant kinds, soils, and water interfaces. Several researchers, such as (Allen et al., 1992; Pauliukonis and Schneider, 2001; Read et al., 2008; Snyder and Boyd, 1987), have utilized this method successfully to estimate ET of entire plants without disturbance from climatic variables. To allow the ET of a wetland to be more attainable for assessment, (Gilman, 1993) recommended erecting barricades to limit lateral subsurface and surface water flows, obviating their inclusion in the hydrological cycle. To accomplish this, a lysimeter, which contains a key section of the desired wetland in a waterproof tank, can be employed. The lysimeter approach is focused on a simplistic water balance formula that allows ET to be calculated utilizing Equation (1).

$$ET = R - \Delta S \quad (1)$$

where: ET is the evapotranspiration in mm/day; R is the rainfall in mm/day, and ΔS is the regular difference in water storage volume inside the lysimeter/day.

Each wetland marsh type had 12 lysimeters mounted in the reed beds of the sea wall reclaimed and unreclaimed marshes Fig 1. Spherical rigid plastic containers with a diameter of 0.55 m and a depth of 1 m were deployed as lysimeters in this research and were mounted by hand. At each chosen spot, a metal rim was drilled into the layer beneath the reeds, water was drained from within the rim, and the sealed reed turves were cautiously split and removed. The content within the ring was then

unearthed, the lysimeter lowered into the resultant cavity, and the ring withdrawn. The excavated soil was then reintroduced into the chamber, with the reed turves removed and confirming the lysimeter's reed bed matched the external reed bed. The lysimeter's tip was placed about 100 mm well above reedbed's top waterline. Each lysimeter was equipped with a flexible hook gauge set between 80 and 120 mm underneath the rim, based on the location and period of the year. At each site, climatological control equipment such as a Grade A evaporation pan (USA) and a rain gauge with a splayed base was installed alongside the lysimeters.

2.2.1. Monitoring regime and successful lysimeters

The following data were reported at every monthly monitoring visit: (1) rainfall; (2) the amount of water needed to fill the evaporation pan and bring the levels of water in every lysimeter up to baseline; and (3) in the lysimeters, the phenological features of reeds and four 0.50×0.50 m static quadrat positions inside the adjoining reed bed for the growing season March–September. According to (ASCE, 1996), lysimetry will only provide appropriate ET measures when the plants' density, height, and leaf area within the lysimeter are similar to the vegetative cover. The quadrants and lysimeters 'Standing Crop' were evaluated to decide which of the lysimeters at every location were 'effective.' Equation (2).

$$MSC = MCH \times MCD \quad (2)$$

Where MSC is mean standing crop ($m \text{ stems}^{-1} m^{-2}$); MCH is mean crop height (m), and MCD is mean crop density ($\text{stems } m^{-2}$).

The 95% confidence mark was calculated using monthly erect crop data, and lysimeters with a crop growth at the maximum limit of the quadrat observations during June and August were regarded as "successful" and subsequently utilized for computing ET rates. Lysimeters within the reed beds of the embankment sea wall reclaimed marshes

were markedly successful since they were devoid of prolonged flooding, excessive shading of the reeds, and seawater water intrusion during high tides. Contrarily, lysimeters outside the seawalls were largely unsuccessful due to exposure to the above factors. Overall, the lysimeters' installation process was successful. Equation (1) was used to estimate $ET_{(Reed)}$ from successful lysimeters.

2.2.2. Leaf area index (LAI) measurement

The leaf area index (LAI) is a unitless metric that characterizes the size of a plant canopy. It is referred to as the one-sided green leaf area per unit land surface area. It plays a crucial role in land-surface systems and climate model parameterizations. Observing the propagation and shifts in the Leaf Area Index (LAI) is critical for determining the growth and longevity of the earth's vegetation. This parameter reflects the amount of leaf material in ecosystems and regulates the biosphere-atmosphere connection via processes including photosynthesis, respiration, transpiration, and rain capture. The (LAI) for this study plants were calculated monthly for eight consecutive months. The leaf area and mass were measured in four quadrat plots for both species. An area meter (LI-3000C Portable Leaf Area Meter LI-COR, Inc., Lincoln, USA) was used to determine the area of the leaves.

2.3. Evapotranspiration (ET) calculation

Monthly meteorological data from 2010 to 2020 were obtained from the nearby automatic weather stations of Yancheng Meteorological Bureau of Jiangsu Province. These include; relative humidity, wind speed, measured pan evaporation, maximum air temperature, minimum air temperature, atmospheric pressure, sunshine hours, soil temperature, and soil heat flux. The modified approach, which enables the calculation of surface resistance using a minimal number of variables that can be quantified in the field Table 1, allows for the estimation of ET in salt marsh ecosystems with limited meteorological data (Gassmann et al., 2019), was used to estimate the open wetland ET rate.

Table 1. Measured data and variables used to calculate the water ET of *S. alterniflora* and *P. australis*.

2.3.1. The Penman-Monteith model

The Penman-Monteith PM equation has been proven to be the most reliable model for estimating ET because of its defined empirical basis and applicability to a wide range of ecosystems (Ma et al., 2016; Yuguda et al., 2020). Bidlake et al. (1996) found an excellent correlation between the PM equation and wetland ET using a fixed surface resistance, whereas the PM equation showed a stronger correlation with measured ET when canopy resistance was varied with season of the year Drexler et al. (2004). The Penman-Monteith formula Monteith and Unsworth (2007) combined the Penman and energy balance equations to solve ET from a well-vegetated surface (Oke and Cleugh, 1987).

$$ET = \frac{\Delta(R_n - G) + \frac{\rho_a c_p (e_s - e_a)}{r_a}}{\lambda \left[\Delta + \gamma \left(1 + \frac{r_s}{r_a} \right) \right]} \quad (3)$$

Table 1

Measured data and variables used to calculate the ET of *spartina alterniflora* and *phragmites australis*.

Variable	Units	Equipment/source
Leaf area index LAI	dimensionless	LI-3000C Portable Leaf Area Meter LI-COR, Inc., Lincoln, USA
Plant height Ph	m	Auxanometer
Open water evaporation E	mm	Class A evaporation pan
Rainfall R	mm	splayed-base rain gauge
Crop coefficient Kc	dimensionless	Lysimeter/open pan evaporation
Reference evapotranspiration ET	mm	Lysimeter

With a steady limitless soil water supply, the plant cover is tolerant of exchanging water vapor with the atmosphere, measured as a resistance r_s . ET is controlled by r_s (m/s) in the Penman-Monteith method.

2.3.2. Surface and canopy resistances

Surface resistance is generated when the plant's leaf stomatal resistance and the resistance of the soil surface combine. Due to the sheer water availability, it is usually assumed that this variable expresses the impacts of soil moisture stress and some other physiological parameters, so wetland surface resistance is likely to be lesser than upland surface resistance. Surface resistance is frequently calculated for crops and grasses using a connection found on LAI, which is proportional to vegetation height. The Penman-Monteith potential and actual ET equations can thus be combined to predict surface resistance r_s Gassmann et al. (2019).

$$r_s = \frac{\Delta(R_n - Q_{G0} - Q_{LE}) + \frac{\rho_a c_p D_p}{r_a} - Q_{LE}\gamma}{\frac{Q_{LE}\gamma}{r_a}} \quad (4)$$

Where Δ is the slope of the equilibrium vapor pressure-temperature function estimated at the air temperature (kPa/ $^{\circ}$ C); R_n is the net radiation ($MJ/m^2/day$); γ the psychrometric constant (kPa/ $^{\circ}$ C); ρ_a is the air density (kg/m^3); c_p is the specific heat at constant pressure (1013 J/ $kg/^{\circ}$ C); Q_{G0} is the surface soil heat flux ($W m^{-2}$); $D_p = (e_s - e_a)$ is the air vapor pressure deficit is the difference between the equilibrium vapor pressure (e_s) and the air vapor pressure deficit (e_a); r_a is aerodynamic resistance (m/s); Q_{LE} is the latent heat flux ($W m^{-2}$); λ is the latent heat of vaporization (MJ/kg). The energy required for warming the air is represented by the difference ($R_n - Q_{G0} - Q_{LE}$). ET (mm) involves the evaporation of free water in instances of dew accumulation. The complete description of the model and other variables is presented in Appendix A.

In addition, Penman-Monteith involves the aerodynamic resistance r_a , was determined as follows:

$$r_a = \frac{\ln \left(\frac{Z_m - d}{Z_{om}} \right) \ln \left(\frac{Z_h - d}{Z_{oh}} \right)}{k^2 U_2} \quad (5)$$

Where Z_m is the height of wind measurements (m); d is zero plane displacement height (m), given as $d = 2/3 h$ for a wide range of vegetation (Allen et al., 1998a); Z_{om} is the roughness length for momentum transfer (m), given as $Z_{om} = 0.123 h$ (Allen et al., 1998b); Z_h is the height of humidity measurements (m); Z_{oh} is the roughness length for vapor and heat transfer (m), can be approximated by $Z_{oh} = 0.1 Z_{om}$ (Allen et al., 1998a); k is the van Karma constant (0.41); U_2 is the wind speed [m/s] at 2 m (For a standardized height for wind speed, temperature and humidity at 2 m, $Z_m = Z_h = 2$ m) (Allen et al., 1998b). Surface resistances more than 1000 m/s (Alfieri et al., 2008; Amer and Hatfield, 2004) and relatively less than 20 m/s (Alfieri et al., 2008) were excluded, in accordance with the minimum r_s threshold for grass, because they correlate to overnight hours when ET is insignificant (Tonti et al., 2020). The parameter r_s is a combined calculation of both processes since ET is the amount of canopy transpiration and soil evaporation. Nonetheless, r_c (m/s) (Leuning et al., 2008) may be used to describe transpiration, dependent on green biomass. (Amer and Hatfield, 2004) suggested the following formula for calculating r_c as a function of r_s and the unilateral LAI:

$$r_c = \frac{0.3LAI + 1.2}{LAI} r_s \quad (6)$$

2.3.3. Crop coefficients estimation Kc (Reed)

The ET rates from a particular environment are determined by the weather prevailing conditions in which the data is obtained. To determine $ET_{(Reed)}$, a systematic technique is necessary for reed bed design. ET data was coupled with standard Reference Crop evapotranspiration (ET_0) data to create a Kc using the methods provided by the FAO

(Doorenbos and Pruitt, 1984), modified in (Allen et al., 1998). Wetland habitat engineers could use the crop coefficients acquired to calculate ET rates from specific habitats employing conventional ET_0 data.

$$K_c = \frac{ET}{ET_0} \quad (7)$$

Where ET is the 10-day measured ET (mm) and ET_0 is the 10-day reference ET (mm).

2.4. Regression analysis

(Wilks, 2011) suggests that ambiguity measures of nonlinear and standard linear regressions can be obtained using just a few variables that quantify the fitness of the model, like the mean square error (MSE) and coefficient of determination (r^2). MSE denotes the variations of the measured ET to forecast (ET^\wedge) value, while in similar units as the predictand, MSE square root (RMSE) reflects the model evaluation ambiguity. The degree of inequality of the correlation defined by the regression is given by r^2 . In this study, the lysimeter measured and estimated ET rates of the reed were compared using simple linear regression analysis. ($ET_{c,u} = u \times ET_{d,u}$) is the equation, where $ET_{c,u}$ is the estimated ET at weather station u (mm month $^{-1}$), $ET_{d,u}$ is the measured ET at the lysimeters (mm month $^{-1}$), and μ_u is the regression coefficient at weather station u . In addition to the regression's determination coefficient, the root mean square error ($RSME_u$) and the Nash-Sutcliffe efficiency coefficient (C_u) at weather station u were determined to evaluate the model's accuracy (Gassmann et al., 2019).

$$RSME_u = \sqrt{\frac{1}{m} \sum_{v=1}^{132} (ET_{d,u,v} - ET_{c,u,v})^2} \quad (8)$$

$$C_u = 1 - \frac{\sum_{v=1}^{132} (ET_{d,u,v} - \bar{ET}_{d,u,v})^2}{\sum_{v=1}^{132} (ET_{d,u,v} - \bar{ET}_{d,u,v})^2} \quad (9)$$

The over bar is an average for the period studied, and the subscript v reflects various monthly values; 132 denotes the number of months from 2010 to 2020.

3. Results and discussion

3.1. Model performance

Two methods were deployed for estimating the ET of the plant species. The first phase is to select a suitable numerical model for calculating ET at nearby estuary weather stations, followed by transferring ET

from nearby weather stations to ET within the lysimeters. Monthly evaporation data from 2010 to 2020 were used to evaluate the efficiency of the Penman-Monteith equation in the first phase. Elementary linear regression indicates that the plant species ET determined using the Penman equation, and the measured value is in good correlation Table 2. For the 12 months of each year, the Penman Monteith equation's RMSE values were all under 16 mm month $^{-1}$. The standard deviations of the estimated monthly ET rate were all less than 10%, with a mean estimate of 1.1%, suggesting a near-flawless estimate. The ET rates were underestimated by the water balance formula and Penman-Monteith equation, with RMSEs of 13.72 mm month $^{-1}$ and 14.85 mm month $^{-1}$ for *P. australis* and 14.72 mm month $^{-1}$ and 13.44 mm month $^{-1}$ for *S. alterniflora*, respectively. The water balance formula and the Penman-Monteith equation have average Nash-Sutcliffe values of 0.83 and 0.88 for all 12 months, suggesting that both methods are compatible. The PM equation proved to be the most accurate model; hence it was utilized to calculate the ET loss in this case.

During the field experiment phases, the average estimated daily ET rate within the lysimeter and at nearby weather stations was 4.21 mm day $^{-1}$ and 3.08 mm day $^{-1}$, respectively. The lysimeter ($ET_{m,ly}$) and nearby weather stations ($ET_{m,ws}$) had a strong agreement in the calculated daily ET rate, according to regression analysis Fig. 2(a,b). A paired-samples *t*-test revealed no discernible differences in daily ET measured within the lysimeter and nearby weather stations. As a result, the ET at nearby weather stations served as appropriate substitutes for what was within the lysimeter. The performance of measured surface resistance r_s^m to calculate water vapor mass fluxes using equation (3) Gassmann et al. (2019) yielded a decent estimate of the ecosystem water vapor exchange. The measured latent heat flux Q_{LE}^M offered the ideal estimation for $ET = Q_{LE}^M/\lambda$ ($r^2 = 0.78$ and RMSE = 84.7 W m $^{-2}$) followed by the computed latent heat flux Q_{LE}^C ($r^2 = 0.74$ and RMSE = 72.4 W m $^{-2}$) for both plant species Fig. 2(c,d).

3.2. Monthly standing crop data

According to field studies, most of the lysimeters, particularly in the unreclaimed marshes, were deemed 'unsuccessful' within the first year of the investigation. This is because the reeds within the lysimeters were not sufficiently established enough. Although there were two successful lysimeters in the unreclaimed marshes in 2019 and three in 2020, probable reed bug invasion and dieback in the reeds made them unsuitable for use in this study since they were not representative of a healthy reed bed habitat. Furthermore, other impediments in the unreclaimed marshes were persistent inundation within the lysimeters, severe shading of the reintroduced reeds, and seawater penetration during high tides. However, in the enclosed seawall reclaimed marshes, five lysimeters were deemed successful in 2019, with seven in 2020. As

Table 2

Comparison of monthly calculated ET and measured ET for both plant species.

Month	<i>P. australis</i>				<i>S. alterniflora</i>			
	Measured ET (lysimeter)		Penman-Monteith model		Measured ET (lysimeter)		Penman-Monteith model	
	Regression equation R^2	C, RSME (mm/month)						
January	$E_c = 1.033E_{ws}$	0.93 14.39	$E_c = 0.945E_{ws}$	0.87 14.38	$E_c = 0.968E_{ws}$	0.87 14.38	$E_c = 0.977E_{ws}$	0.75 14.39
February	$E_c = 0.876E_{ws}$	0.78 13.82	$E_c = 0.987E_{ws}$	0.67 15.16	$E_c = 0.975E_{ws}$	0.67 13.06	$E_c = 0.965E_{ws}$	0.76 13.92
March	$E_c = 0.950E_{ws}$	0.92 14.76	$E_c = 0.971E_{ws}$	0.58 15.85	$E_c = 0.968E_{ws}$	0.89 15.86	$E_c = 0.951E_{ws}$	0.83 14.76
April	$E_c = 0.911E_{ws}$	0.75 13.70	$E_c = 1.07E_{ws}$	0.77 12.47	$E_c = 1.065E_{ws}$	0.76 13.67	$E_c = 1.045E_{ws}$	0.87 13.57
May	$E_c = 1.114E_{ws}$	0.67 12.98	$E_c = 0.929E_{ws}$	0.79 11.74	$E_c = 0.961E_{ws}$	0.78 12.74	$E_c = 0.961E_{ws}$	0.97 13.80
June	$E_c = 0.893E_{ws}$	0.68 14.19	$E_c = 1.058E_{ws}$	0.76 13.20	$E_c = 1.098E_{ws}$	0.74 12.20	$E_c = 1.058E_{ws}$	0.79 14.29
July	$E_c = 1.090E_{ws}$	0.91 12.43	$E_c = 1.078E_{ws}$	0.87 13.41	$E_c = 1.044E_{ws}$	0.73 14.39	$E_c = 1.049E_{ws}$	0.84 13.55
August	$E_c = 1.024E_{ws}$	0.74 11.69	$E_c = 0.923E_{ws}$	0.77 11.28	$E_c = 0.913E_{ws}$	0.85 12.28	$E_c = 0.987E_{ws}$	0.78 13.96
September	$E_c = 1.003E_{ws}$	0.92 13.66	$E_c = 1.099E_{ws}$	0.86 12.79	$E_c = 1.076E_{ws}$	0.89 12.97	$E_c = 1.075E_{ws}$	0.85 13.58
October	$E_c = 1.128E_{ws}$	0.82 15.28	$E_c = 0.915E_{ws}$	0.84 15.87	$E_c = 0.907E_{ws}$	0.74 15.87	$E_c = 0.992E_{ws}$	0.82 15.24
November	$E_c = 0.858E_{ws}$	0.84 10.44	$E_c = 0.975E_{ws}$	0.79 10.76	$E_c = 0.958E_{ws}$	0.86 13.65	$E_c = 0.926E_{ws}$	0.79 13.59
December	$E_c = 1.017E_{ws}$	0.76 13.30	$E_c = 0.965E_{ws}$	0.87 14.12	$E_c = 0.956E_{ws}$	0.79 12.55	$E_c = 0.953E_{ws}$	0.89 14.46

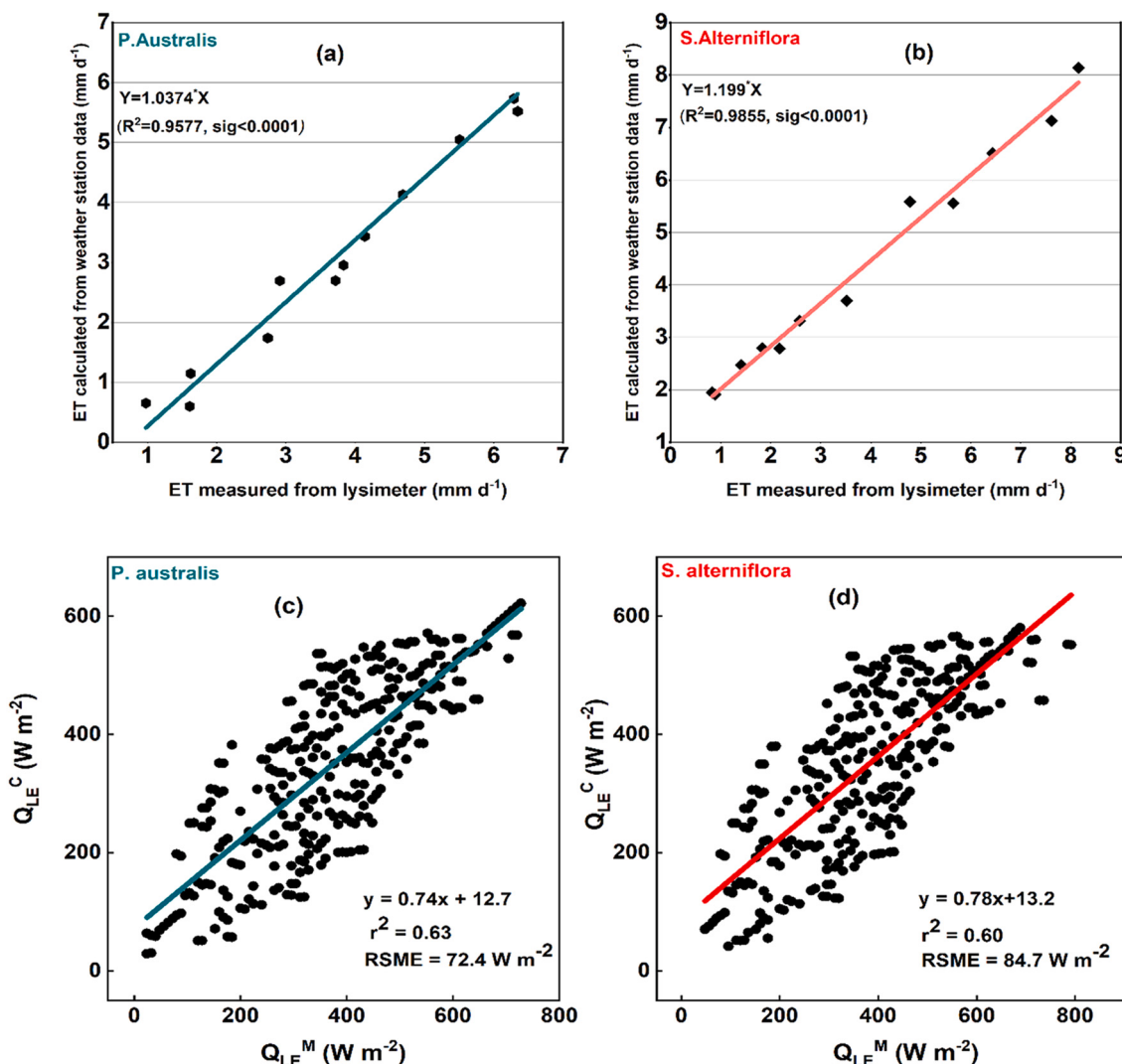


Fig. 2. Regression analysis of compared monthly measured and calculated (a,b) open water evaporation at the lysimeter and automatic weather station, (c,d) latent heat flux for both plant marshes.

mentioned above, lysimeters with a standing crop inside the transect, data limits from June to August were deemed 'successful' and utilized in ET rate calculations. Both native and invasive plants reached a

maximum height in July, with a mean monthly standing crop of 96.38 ± 4.93 plants m⁻² and 107 ± 5.07 plants m⁻², respectively, during the peak of the growing season Fig 3(a,b).

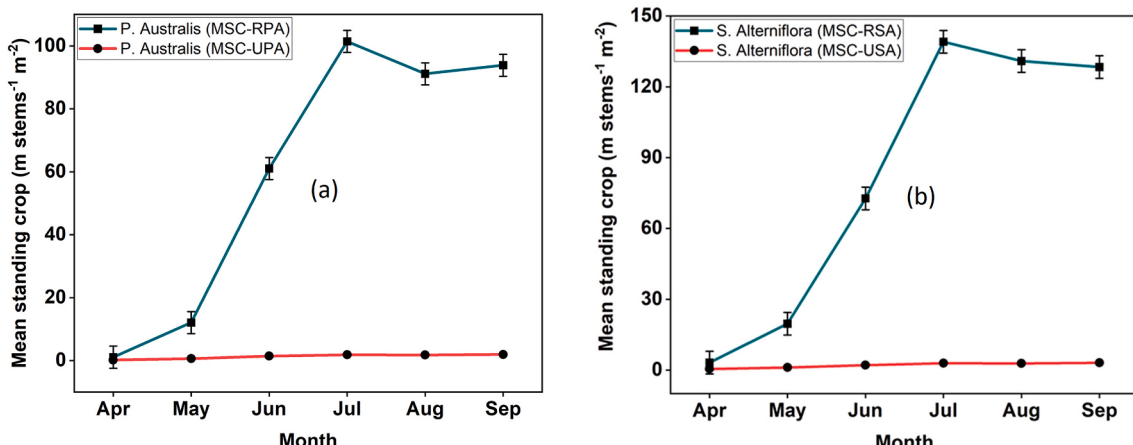


Fig. 3. Monthly standing crop data from the quadrants (a) mean standing crop MSC in the seawall reclaimed *P. australis* marshes RPA and unreclaimed *P. australis* marshes UPA (b) mean standing crop MSC in the seawall reclaimed *S. alterniflora* marshes RSA and unreclaimed *S. alterniflora* marshes USA.

3.3. Relationship between ET and ecophysiological factors

Both species' LAI exhibited substantial seasonal variations, with more outstanding scores in the summer Fig. 4(a,b). There was a notable difference between the two species, with *S. alterniflora* having a higher mean LAI (1.9–6.8) than *P. australis* (0.5–5.1), particularly in the second phase of the crop growing season. The photosynthetic season of *S. alterniflora* was longer than that of *P. australis*. However, the timing of

shoot emergence in the spring was nearly identical for both. *S. alterniflora* matured somewhat longer than *P. australis* at the end of the growing season. *S. alterniflora* had a high LAI in December, while *P. australis* had a relatively low LAI in October. The relationship between ET aggregation and plant height and leaf area index is shown in Fig. 4(a, b,c,d) for various months. In September, *P. australis* continued to sprout. When the plant's height increases marginally, the leaf area index somehow doesn't change significantly, but ET rises slightly. The

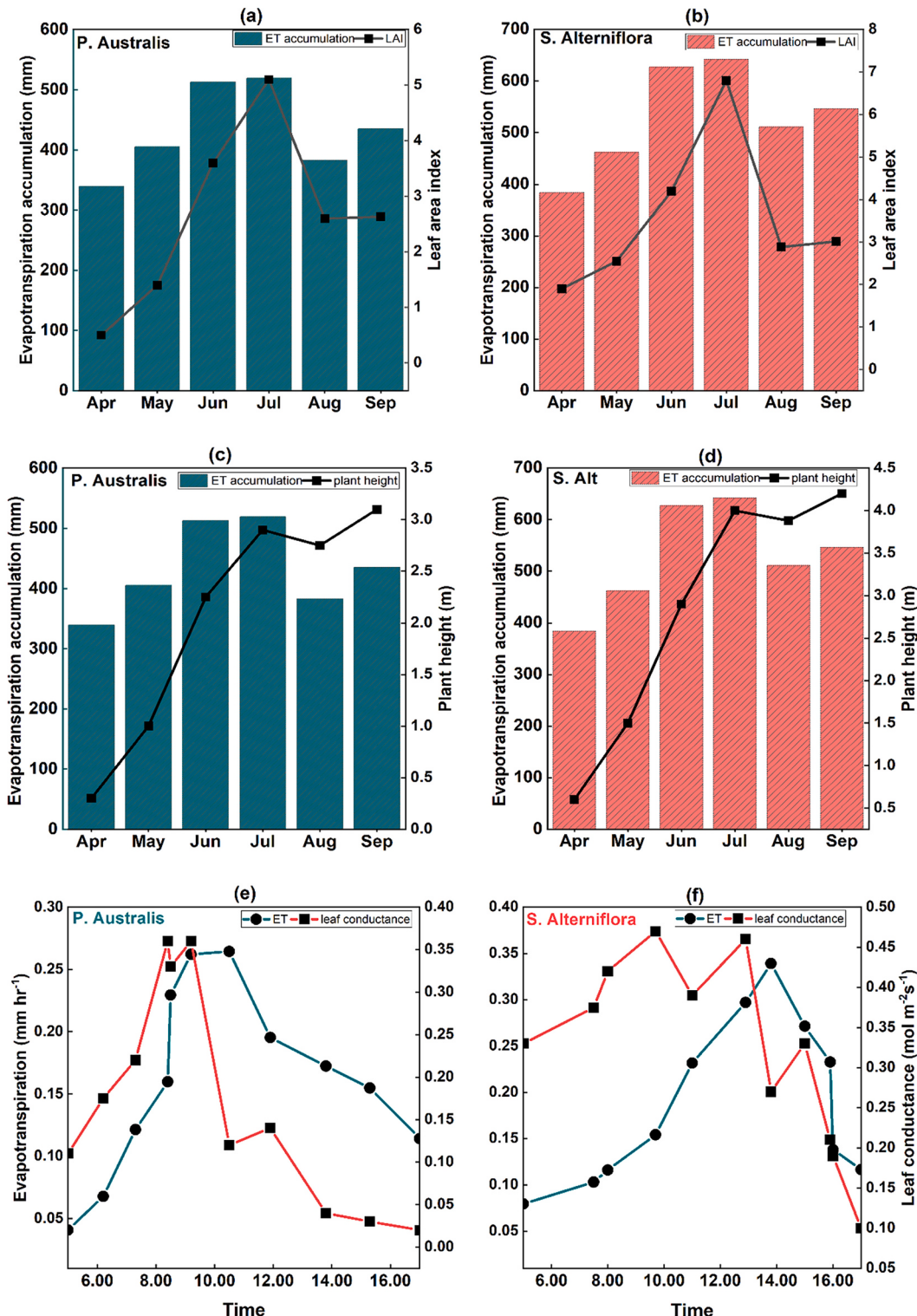


Fig. 4. Relationship between evapotranspiration accumulation and (a,b) LAI (c,d) plant height and (e,f) leaf conductance for both plant species.

correlation coefficients between plant height and ET are 0.524 and 0.643, respectively, while the correlation coefficients between LAI and ET are 0.728 and 0.802, suggesting that plant height and leaf area index have a major impact on ET.

Besides physical environmental influences, photosynthesis, leaf shape, and stomata feature impact ET in both plant communities. In June, the correlation between ET and stomatal conductance is shown in Fig. 4(e,f). Lesser values at dawn and dusk and increasing values at noon are observed in leaf stomatal conductance and ET. For *P. australis* and *S. alterniflora*, the correlation coefficient between stomatal conductance and ET is 0.89 and 0.92, respectively, demonstrating that stomatal conductance has a considerable impact.

3.4. Responses of ET to environmental factors

Fig. 5(a,b) shows the correlation studies between ET and its environmental components based on data from the growth season (April 22 to October 28) and non-growing season (January 1 to April 21) of 2019. Net radiation, air temperature, and relative humidity have a significant impact on evapotranspiration in both the growing and non-growing seasons, while wind speed is only relevant in the non-growing season. Each factor does not interact separately; hence a single variable connection could only assess the effectiveness of one variable that has an effect on ET. Multiple stepwise regression analysis is effective for more properly analyzing the link between environmental conditions and ET.

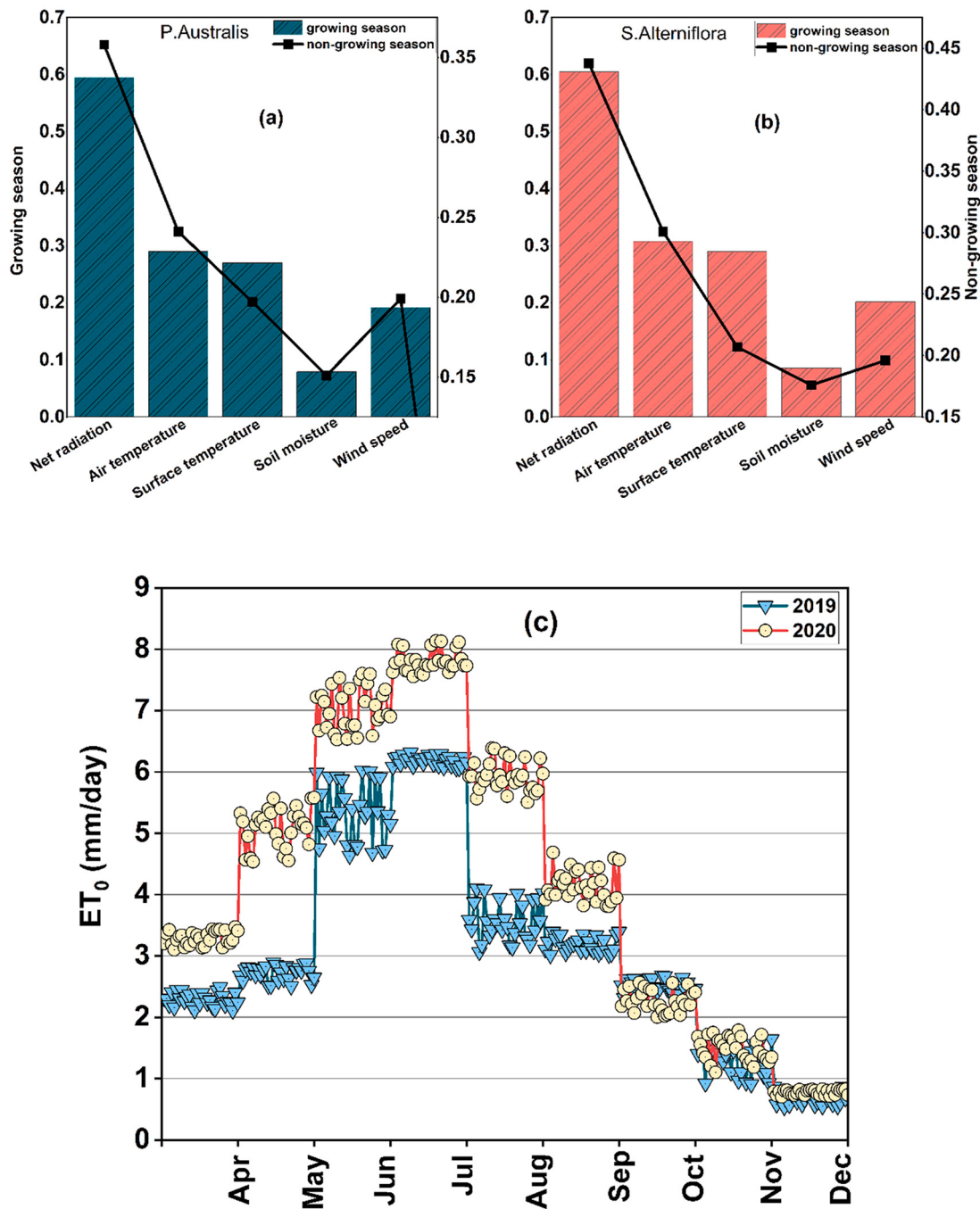


Fig. 5. Relationships between (a,b) environmental factors and ET of both plant community (c) ET₀ daily rates during 2019 and 2020 observation periods.

Based on data from the growing and non-growing seasons, Table 3 illustrates the results of a correlation analysis between ET and its environmental components. Net radiation, soil moisture, relative humidity, air temperature, and surface temperature are the primary parameters during the season of growth, according to stepwise regression analysis. The multiple correlation coefficient is 0.712 for the plant community. The F test ($F \leq 0.05$) reached extraordinary levels, indicating that ET is closely linked with environmental parameters and is a synthetic depiction of the wetland microclimate. Net radiation, surface temperature, and wind speed are all aspects to consider during the non-growing season. The multiple correlation value is 0.436, while the F test ($F \leq 0.05$) is exceptional. According to stepwise regression analysis, net radiation is the key predictor and impetus on ET of the Phragmites and spartina communities throughout growing and non-growing seasons.

3.5. Evapotranspiration (ET) rates

ET data for planted lysimeters in each of the experimental sites were averaged to generate monthly mean ET values over the relevant research periods, after which all data were pooled to give site-specific mean monthly values. The analysis excludes monitoring periods during which lysimeters were exposed to overflowing due to significant rain or floodwater inundation. Generally, the ET rate rises dramatically between May and June, with peak rates occurring between June and September. Although daily ET patterns were comparable throughout the investigation period, excluding the first week of June through the last week of July, the 2019 ET₀ mean value (3.80 mm/day) were typically lower than the 2020 ET₀ values (4.11 mm/day) due to higher temperatures and lower relative humidity Fig. 5c. Daily seasonal peak ET was similar for both plants on average: 6.35 mm/day for *P. australis* and 8.16 mm/day for *S. alterniflora*. During the monitoring period, daily ET values ranged from 0.98 to 6.35 mm/day and 1.91 to 8.16 mm/day respectively, in both plants; the least average monthly ET values were 0.98 mm/day and 1.91 mm/day in November (fall). The highest was 6.35 mm/day and 8.16 mm/day in July (summer). With daily control evapotranspiration ET_{con} values ranging from 1.65 to 3.63 mm/day in 2019 and 1.74 to 3.66 mm/day in 2020, the 10-day average ET_{con} showed trends that matched pretty closely the 10-day average ET₀ (3.08 mm/day in 2019 and 3.18 mm/day in 2020). Both plants had identical cumulative ET_{con} (756 mm and 863 mm), around 10% less than the total ET₀ for the growing season Fig 6 (a,b).

The daily change of ET between the growing and non-growing seasons is depicted in Fig. 7 (a,b,c,d). Observations indicate that ET is substantially lower at night; when the temperature rises, the ET rate rises as well, peaking between 12:00 and 14:00. As a result, the ET rate continuously falls as the temperature drops, and it is lowest at night. These findings show that daily ET fluctuation throughout months followed the same single-peak curve pattern, with lower amounts at dawn and sunset but greater rates at noon. Daily ET changes throughout the non-growing season, however, exhibited a pattern of lower levels in the

Table 3

Regression analysis between environmental factors and evapotranspiration of Plant community.

	Growing season	Non-growing season
Control factor	Radiation, soil moisture, relative humidity, air temperature and surface temperature	Radiation, surface temperature and wind speed
R	0.712	0.436
F	899.205	256.564
Sig.	0.000	0.000
Regression equation	$LE = 0.273R_n + 60.202w + 0.263H_s + 2.036T_a - 1.609Ts - 21.733$	$LE = 0.043R_n + 0.277T_s + 0.391w + 5.829$

NB: LE is evapotranspiration, R_n is net radiation, w is soil moisture, H_s is relative humidity, T_a is air temperature and Ts is surface temperature.

dawn and dusk and higher amounts towards midday, without any peak curve. Due to transpiration, monthly ET accumulation fluctuates more during the growing season (April to October) and less over the non-growing season (November to March) due to limited evaporation Fig. 7(e,f). Because of the impact of precipitation, the ET rate diminishes in August.

Over the entire investigation period, *S. alterniflora* had the uttermost average ET value (8.15 mm/day) across the whole period. Compared to studies that deployed lysimeters in the field, (Dacey and Howes, 1984) obtained a total ET of 160.8 ml/day against a water uptake of 202.32 ml/day for *S. alterniflora*. The highest average ET value of *P. australis* (6.35 mm/day) compared to other lysimeter studies is entirely on par with 2.94–6.30 mm/day and 10–12 mm/day (Fermor et al., 2001; Smid, 1975) and much little less than 17.9–27.8 mm/day by (GAVENCIAK, 1972). Our highest average ET value is also much less compared to average ET values of constructed wetland *P. australis* plants (16.87 mm/day and 17.31 mm/day) found by (Rozkošný and Šálek, 2006) and (Milani et al., 2019). It is entirely within the range of those obtained in other constructed wetland investigations executed in temperate regions, with ET ranging from 0.2 to 10.6 mm/day (Chazarenc et al., 2003; Fermor et al., 2001; Headley et al., 2012; Herbst and Kappen, 1999; Milani and Toscano, 2013). On the other hand, a Pilot CW In the two experimental sites found an average *P. australis* ET of 30.9 mm/day (Borin et al., 2011), while (El Hamouri et al., 2007) discovered a *P. australis* ET rate of roughly 57 mm/day in a horizontal underlying wetland in Morocco. Both are relatively higher than the averages found in this study.

Further employing lysimeters in both fertilized and nearby unfertilized grass stands, (Howes et al., 1986) found that the loss of pore-water by ET in stands of short *S. alterniflora* in the field is about $1\text{ m}^{-2}\text{ d}^{-1}$. The disparity is most probably due to a plant water shortage that existed prior to the start of the experiment. Range of (3.12–12.48 mm/day) for the open-water lysimeters for a *S. alterniflora* dominated saltmarsh (ET) and pan evaporation (E) suggest that, although reduced crop densities may not significantly contribute to atmospheric water loss, water transport pathways and solute concentration trends in the subsurface environment differ from those found in a tidal freshwater marsh (Hussey and Odum, 1992). For Piezometers, (Hughes et al., 2012) investigated the relationship between hydrologic variability and changes in marsh subsoil conditions that could be detrimental to the salt marsh grass *S. alterniflora*, and obtained an average ET rate of (1–6 mm/day). Employing the Cut-stem weight changes technique, ET for *P. australis* ranged from as low as 2.23 mm/day to as high as 13 mm/day (Królikowska, 1971; Smid, 1975). Bowen ratio technique found a value of 6.9 mm/day in July (Smid, 1975), and 6.4 mm/day was found adopting the Mass water balance approach (Burgoon et al., 1997), all on par with the average for this study. Utilizing direct ET measurements, from eddy covariance method, ET rate peaked at 3.84 mm/day in a mesotidal system dominated by *Spartina alterniflora* in the low marsh (Mariotti et al., 2019). In comparison, it ranged from 3.4 to 3.7 mm/day over a *P. australis* reed marsh in Northeast China from 3-year data (Zhou et al., 2010). Based on simulation and field sampling experiments, (Zhao et al., 2012) and (Zhou and Zhou, 2009) obtained daily ET rate ranges of 2.70–5.93 mm/day and 0.1–5.8 mm/day, respectively, for *P. australis*, which is very much correlative to the range obtained in this study. The variations in methodology, location, and sampling frequency make absolute comparisons of these ET rates impractical.

3.6. Crop coefficients

The trapezoidal form of Kc for crop plants (Allen et al., 1998a), which represents the four seasonal developmental stages for both *P. australis* and *S. alterniflora* species, is comparable to the crop coefficient temporal patterns Fig 6(c,d), (initial stage, developmental stage, middle, and season end). In the early stages of growth, the 10-day Kc for both species ranged from 0.77 (*P. australis* in the second 10 days of May)

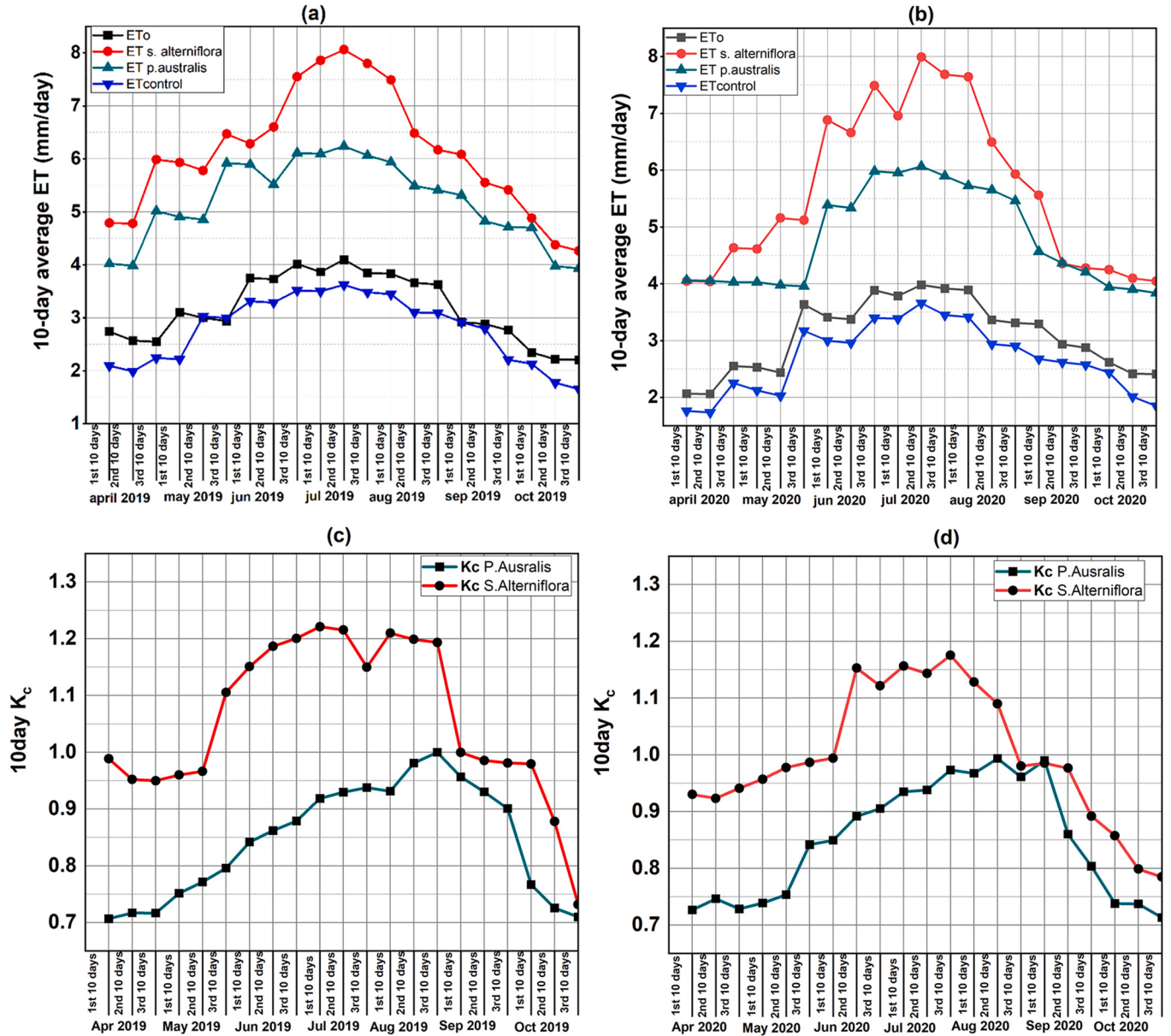


Fig. 6. Trend of meteorological data and average 10-day ET_0 , ET_{con} , ET for *S. alterniflora* and *P. australis* during 2019 (a) and 2020 (b), Kc 2019 (c) and Kc 2020 (d) observations.

to 1.11 (*S. alterniflora* in the last ten days of May). Based on species type and season, the crop growth stage lasted different amounts of time: From the first week of June to the second week of August, *P. australis* had the lowest duration of 10 weeks, while *S. alterniflora* had the most prolonged period of 13 weeks, from the first week of June to the first week of September. The 10-day Kc of *P. australis* ranged from 0.77 to 0.80 in *S. alterniflora* during the crop development. In the mid-season, *P. australis* achieved the highest 10-day mean Kc value (0.97), whereas *S. alterniflora* had Kc of (1.21). The 10-day Kc dropped during plant withering (late season) to the end of November, during which the mean values for the season were around 0.37 for *P. australis* and 0.65 for *S. alterniflora*.

As illustrated in Fig. 8 (a,b), the 10-day Kc value for *P. australis* and *S. alterniflora* obtained in 2019 and 2020 had a positive correlation, according to linear regression. This is attributable to the significant variations in biomass characteristics between the two years, as *P. australis* had a higher linear regression than *S. alterniflora*. Linear regression analysis further revealed that 10-day Kc was substantially

linked with the phenological indicator (plant height), with a correlation value ranging from 0.87 (*P. australis*) to 0.72 (*S. alterniflora*) Fig. 8 (c,d).

The results reported in both plant types demonstrated a strong link between the extent of the wetlands and ET. Other investigations (Fermor et al., 2001; Peacock and Hess, 2004; Read et al., 2008; Zhou and Zhou, 2009) observed ET rates of between 0.5 and 5.8 mm day⁻¹ and average Kc readings of around 0.53 and 1.09 for *P. australis* in coastal wetlands covering between 235 and 90,000 ha, respectively. These findings are consistent with ET rates of 0.60 to 6.35 mm/day and mean Kc of 0.77 for *P. australis* found in this study. Unfortunately, due to a lack of research on the subject, it was impossible to present comparison Kc values for *S. alterniflora* from other natural or constructed wetlands. However, based on reference ET values obtained by synthesizing flux and climatological observations from numerous eddy covariance variability sites across China (Xiao et al., 2013), Kc for *S. alterniflora* was extrapolated in conjunction with measured ET values from this study. Kc values of 0.77 for this study and 0.80 (extrapolated) indicate consistency and strong correlation in approaches. As such, Wetland ecosystem planners can use

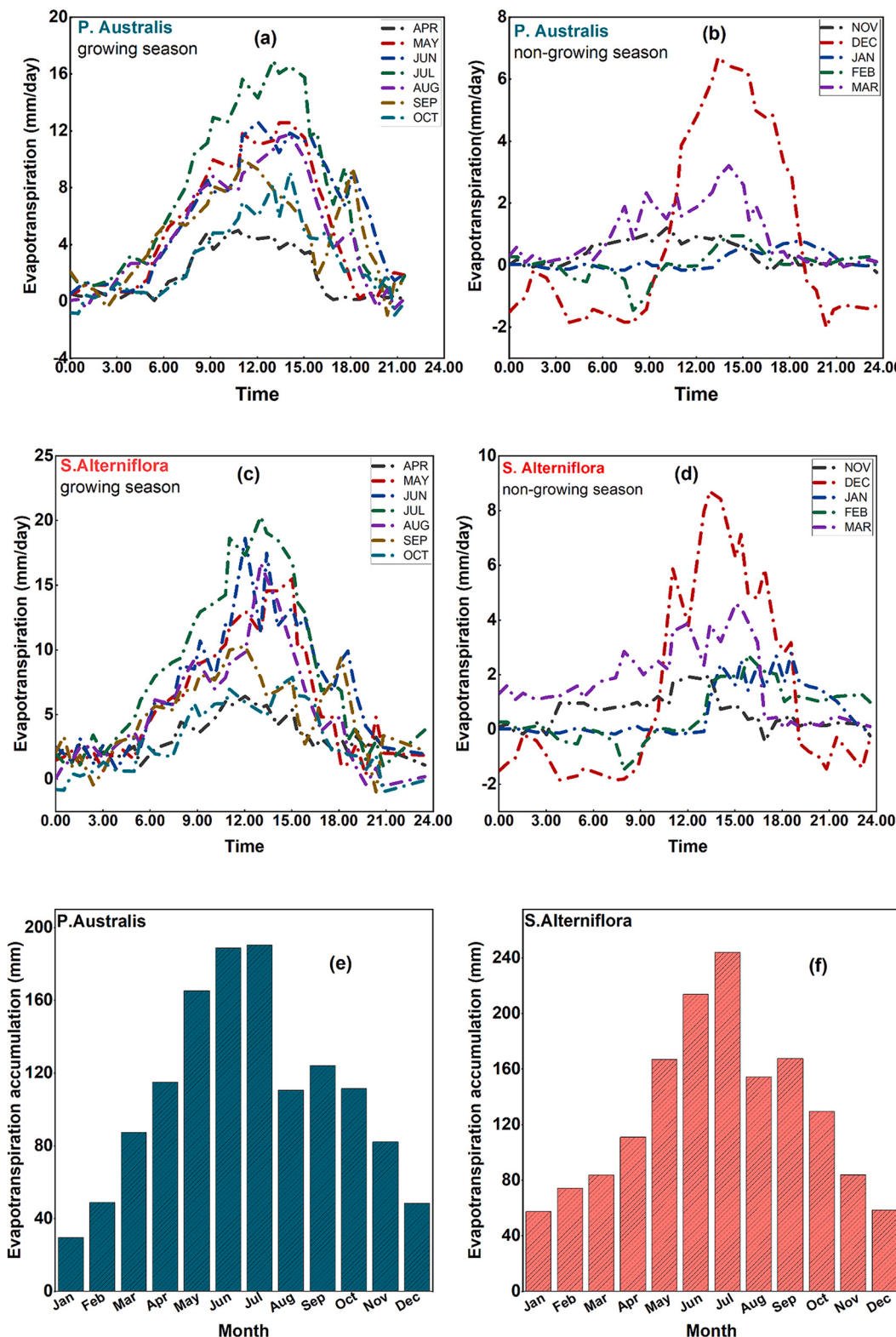


Fig. 7. (a,b) daily evapotranspiration dynamics of *P. australis* community (c,d) daily evapotranspiration dynamics of *S. alterniflora* community (e,f) monthly evapotranspiration accumulation of both Plant community.

these crop coefficients acquired to calculate ET rates from target habitats utilizing standard ET_0 data.

3.7. Invasive water loss dissimilarities between leaf and plant scale

ET is related to vegetation physiology because stomatal conductance, which symbolizes the control of the leaf stomata on water vapor flow, influences transpiration (Dolman and Miralles, 2014; Eichelmann et al.,

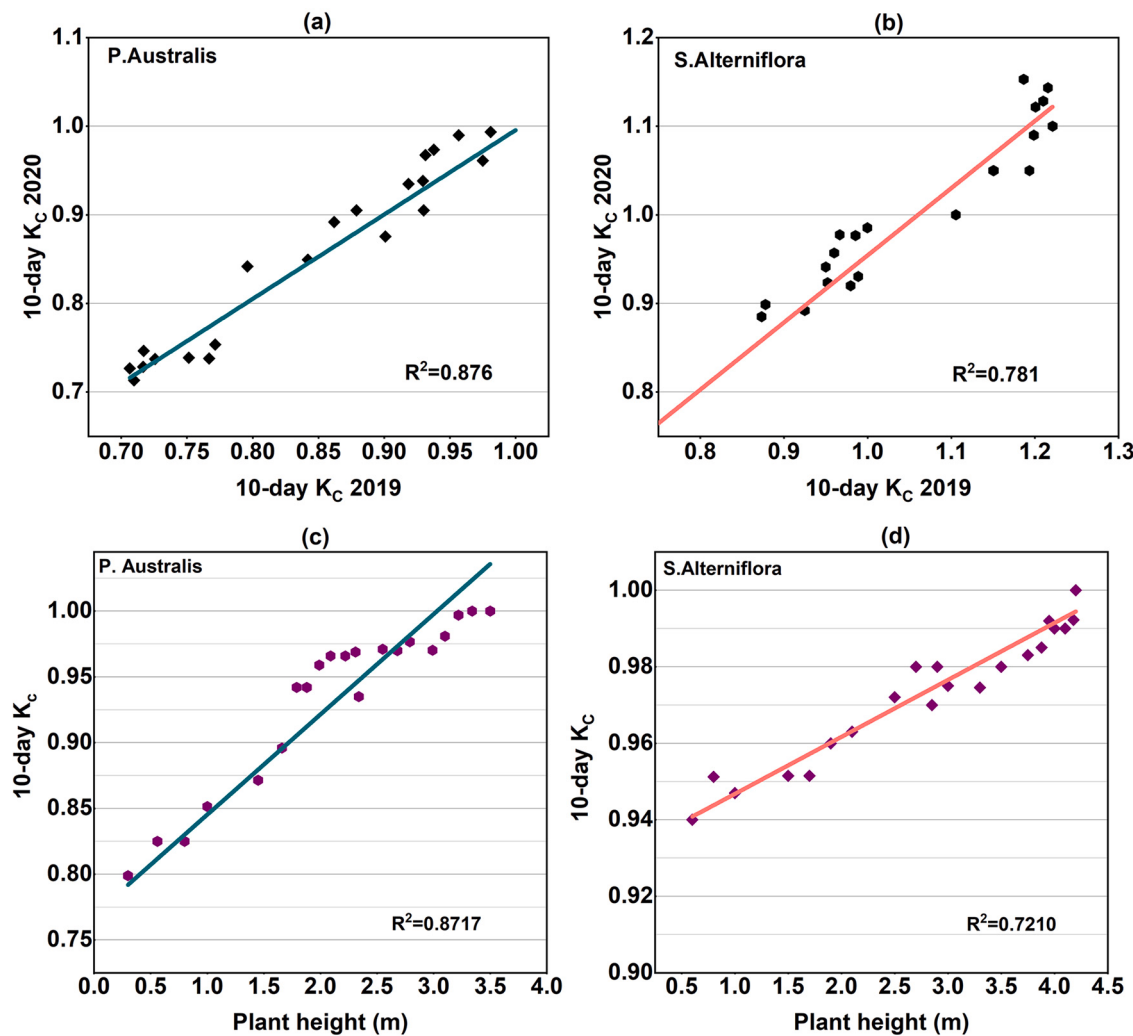


Fig. 8. (a,b) relationship between 10-day crop coefficient K_c (c,d) relationship between 10-day K_c and plant height for *P. australis* and *S. alterniflora* during 2019 and 2020 observations.

2018; Funk and Zachary, 2010). This is why at the leaf scale, invasive species can utilize water more quickly than native species (Cavaleri and Lawren, 2010; Zeballos et al., 2014). In this study, invasive *S. alterniflora* plants used more leaf-scale water than native *P. australis* plants. Findings also demonstrated larger overall stomatal conductance for invasive plants, a pattern paralleled in photosynthetic capacity, showing a trajectory of relatively higher metabolic rates for invasive *S. alterniflora* comparative to co-existing native *P. australis* of similar growth structure. Investigations have demonstrated commonly invasive species to exhibit increased photosynthetic activity, which for C_3 species is highly tied to a loss of water from stomata. An increase in plants' stomatal conductance due to photosynthetic nitrogen-use efficiency and water-use efficiency WUE tradeoffs may raise CO_2 interstitial levels, resulting in increased photosynthesis without a difference in nutrient content but an increase in water dissipation off the leaf (De Gong et al., 2018; Reich et al., 1989). These findings corroborate those of global meta-analysis, which indicated that invasives have higher foliar nitrogen concentrations and photosynthetic rates on average than natives (Jiang et al., 2009; Leishman et al., 2007). Invasive species and natives were both shown to exhibit higher intrinsic and immediate WUE. While disparities in intrinsic and immediate WUE between species can be explained by changes in environmental factors that may include leaf phenology (Seibt et al. 2008), the differences found in our investigation were attributable to disparities in community structure since each invasive or native duo

co-occurred in similar external conditions. Our findings matched research in Hawaii that examined 19 taxonomically linked native/invasive plant species pairings (Funk and Vitousek, 2007). However, they contradicted the common perception that invasive species favored quicker rates of growth due to resource efficiency (Grotkopp et al., 2002).

The increased summer ET potential trend in invasive *S. alterniflora* Fig. 7 (e,f) could be due to a variety of factors such as; (i) *S. alterniflora* has a WUE of over 25% higher than *P. australis* (Jiang et al., 2009), explaining why invasive species may tolerate drier microsites or consume more water, leading the soil near their roots to dry out faster than native species. (ii) Due to considerable seasonal fluctuations in the overall pattern of SLA between invaders and natives, the quantum yield of *S. alterniflora* was roughly 10% higher than that of *P. australis*. (iii) During the day, photosynthetically active radiation and vapor pressure deficit had the most influence on ET, whereas, at night, wind speed and friction velocity governed ET variability. All through the growing season, *S. alterniflora* had considerably greater maximal net photosynthetic rates and day respiration than *P. australis*, except for October (Jiang et al., 2009). However, because the stomata of plants close about noon in the summer, there may be a higher transpiration proportion of ET_0 in the winter than in the summer (Dzikiti et al., 2016; Yu et al., 2008b). Invasive species' lower predawn water potential may also signal higher night-time transpiration, a feature that is gaining more research

attention (Dawson et al., 2007). Despite continuously diminishing conductance in both species, the daily patterns of net photosynthesis were preserved. Leaf conductivity decreased with rising temperature during all periods studied in conjunction with these monitoring investigations (Drake et al., 2018; Mathias and Thomas, 2021).

As ambient temperature and sunshine increased throughout the day, this broad conductivity variation was most likely due to lower xylem osmotic pressure and growing vapor pressure differentials (Goto et al., 2021; Höltsä et al., 2018). Even though there could be more than enough water in the root zone, stomata must close to avoid xylem cavitation (Dzikiti et al., 2016). Stomatal closure can also result when the root water absorption does not balance the transpiration requirement there at evaporating spots in the leaves owing to excessive atmospheric evaporative demand. It could also be caused by high hydraulic resistance in the transpiration stream (Dzikiti et al., 2007). In the case of drought resistance and water use tradeoffs, invasive plants were pretty resistant to cavitation in stem xylem conduits, kept their leaves, and had good leaf osmotic adjustment. In contrast, native saplings had xylem cavitation, prominent leaf loss, and much less efficient leaf osmotic adjustment (Pintó-Marijuan and Munné-Bosch, 2013). The comparatively high rates of ET in the taller *S. alterniflora* stands were mirrored by comparatively high rates of significant water loss, both in leaf area Fig. 4(a,b) and marsh surface area (Giurgevich and Dunn, 1982).

S. alterniflora's WUE is likewise higher than that of *P. australis* and several other native species because the main effect of salt stress is water deficit since plants living in salt marshes require a higher WUE. The significantly higher water loss rates may be necessary for keeping the leaf temperature around the seasonal photosynthetic peak (Hester et al., 2001; Jiang et al., 2009). However, in this study, *S. alterniflora* exhibited a higher specific leaf area SLA than *P. australis*, which corroborates the typical association between invaders and native species. One of the morphometric characteristics that influence transpiration water loss is SLA. A lower SLA lengthens the distance water must flow out of the leaf, resulting in water-saving (McDowell, 2002; Van den Boogaard and Villar, 1998). As a result, *S. alterniflora*'s higher SLA may have contributed to its enhanced WUE and resulted in *S. alterniflora*'s higher salt tolerance (Jiang et al., 2009; Wang et al., 2006). Trends of differences in water loss were comparable to the seasonal shifts in both air temperature and ET. Net photosynthesis rates in the shorter *S. alterniflora* were consistently lower than those in Taller *S. alterniflora* at both the immediate and daily levels. For both height types of *S. alterniflora*, the seasonal dynamics of ET to environment conditions were equivalent, according to (Giurgevich and Dunn, 1979), but that Taller *S. alterniflora*'s absolute ET rates were regularly higher than the shorter. The distinction in net photosynthesis rates between the height forms of *S. alterniflora* is most likely due to a combination of higher salinity, lower nitrogen availability, and complexity of attributes linked with the shorter *S. alterniflora* community's anaerobic, poorly drained soil conditions (Giurgevich and Dunn, 1979; Linthurst and Seneca, 1980; Mendelsohn and Seneca, 1980). The rates of daily water loss from *S. alterniflora* were equivalent to or somewhat higher than the national average. On a leaf area basis, they are higher than *P. australis* Fig. 4(a,b, e,f), although the rate could be substantially lower (Giurgevich and Dunn, 1982).

Due to the significantly reduced levels of leaf biomass in the shorter plant community, less water was transpired. However, the fluctuation in ET is greatly influenced by environmental factors, including net radiation vegetation, which has a substantial impact on the ET of *P. australis* communis, particularly the LAI and leaf conductance (Yu et al., 2008a). The decreased levels of leaf conductance and net ET in *P. australis* during the warmer months were due to the temperature constraint of net photosynthesis. Higher transpiration rates were possible because of cooler air temperatures in the spring and fall. Even though actual rates of ET in *P. australis* were comparable to those in *S. alterniflora* on a leaf area basis, leaf inclination and a lower LAI, rendered this species incapable of adapting to the high ambient photosynthetically active photon

flux density as well as *S. alterniflora*. As a result, the net primary productivity of *P. australis* was lower than *S. alterniflora*'s (Jiang et al., 2009). Nonetheless, water loss in *S. alterniflora* was often higher than in *P. australis*, in leaf area and, more importantly, leaf weight Fig. 4(a,b). The *P. australis* community's substantial stock of leaf biomass culminated in predicted water loss rates per marsh surface area that was more than the shorter *S. alterniflora*, but comparable in volume and distribution to the taller *S. alterniflora* also had a significant LAI and leaf biomass.

The absolute rates of ET provide a better assessment of intrinsic variations in plant water-use strategies. The increased WUE trends in *S. alterniflora*, a C₄ species, were mainly attributable to better substrate conditions that allowed for higher ET rates. Even though shorter *S. alterniflora* exhibits C₄ photosynthesis, the increased salinity, and reduced nitrogen distribution in the highly vegetated community resulted in a significant curtailment of ET in the shorter *S. alterniflora* stands and a lower WUE (Giurgevich and Dunn, 1982). Since the rates of transpiration in Taller and Short *S. alterniflora* stands were identical, the rates of ET in both height forms change the water use. Despite having comparatively high rates of net photosynthesis, *P. australis*, a C₃ species, had inherently high transpiration rates, resulting in lower water use in this species. Although they thrive with a steady water supply, wetland plants' adjustment of stomatal openings in response to microclimatic fluctuation may have led to the observed differences in ET. As such, native plants, especially perennial species, are positioned to gain from having more robust stomatal control and rhizome systems to improve nutrient uptake than annual plants (Prieto et al., 2018; Tordoni et al., 2019).

3.8. Invasive plant water use at the ecosystem scale and implications for global climate change

Several ecosystem services rely on the volume and availability of freshwater. By their phylogenetic behavior and relationships with other species, invasive plants can diminish hydrological services, exacerbated when invasive species are ecosystem engineers or transformers (Catford, 2017). The ecosystem develops a severe scale dependency for the water usage comparisons between invasive and native species when the flow of water from leaf to plant and plant to plant is disrupted. Distinctions in phenology between native and invasive plants, like the onset of leaf flushing or senescence, can potentially lead to invaders consuming a large amount of water at the ecosystem scale (Calder and Dye, 2001). Despite observing that invasive-dominated areas have markedly higher capillary flow per surface area than native-dominated areas, we did not notice this tendency in ET, due to limited available data at this spectrum. This disparity may occur when, unlike ET, daily capillary flow per unit surface area typically ignores canopy interception and undergrowth water usage, both of which can contribute to a significant portion of overall rainfall reverted to the atmosphere (Kagawa et al., 2009; Le Maitre et al., 1999). Ecosystems dominated by invasive species and native species of the same development form had an equal chance of having immense ET when incorporated into differential growth. Invasive-dominated ecosystems tended to take on new forms and have a higher ET Fig. 4(a,b,c,d,e,f) & Fig. 7(e,f), which is mainly due to instances of invading herbaceous habitats by arboraceous species (Farley et al., 2005; Huxman et al., 2005). Furthermore, invasive alien plants may induce increased ET in native communities, with the effect becoming more pronounced as the number of invasive propagules expands (Tang et al., 2020).

This occurrence could be caused by a number of factors, including (1) Invasive species are taller and have a rougher aerodynamic than native species, with increased precipitation interception and canopy linkage (Farley et al., 2005; McNaughton and Jarvis, 1983); (2) the thicker the biomass cover, the more water use; (3) invasive species have deeper roots, allowing them to maintain transpiration under dry conditions (Calder and Dye, 2001); (4) Shrubby flora often senesces earlier and has a shorter transpiration period than other types of vegetation

(Calder and Dye, 2001); and (5) invasive interference may enhance soil surface evaporation and therefore ET.

ET of invasive-dominated ecosystems appeared to surpass native ET where conditions were wetter and hotter Fig. 5(a,b,c) and Fig. 7(a,b,c,d,e,f). Plants have a significantly greater impact on the water balance in humid regions because precipitation surpasses potential ET. In contrast, much water evaporates regardless of vegetation in arid areas where precipitation does not exceed potential ET (Huxman et al., 2005). The differences in water uptake patterns identified in native and invasive plants suggest that invasives may have the edge over native species that are physiologically disturbed due to belowground inundation during the rainy season (Ewe and Sternberg, 2002). Our findings contradict a study that claimed invasive trees produce a higher rise in water demand in arid climates (Calder and Dye, 2001) and another worldwide meta-analysis that concluded that afforestation has a bigger relative impact on hydrology in tropical areas (Farley et al., 2005). These differences could partly be attributed to the hotter biomes in our study in which wetter temperatures had invasive species displacing native grass species, whilst the drier ecosystems had species with similar growth forms Fig. 5(a,b,c).

While our research shows that plant invasion has negative implications for water use, particularly in the present worldwide environmental climate, as well as the growing acknowledgment of the role of ecological systems and carbon capture. This water-carbon tradeoff underpins species metamorphosis must be taken into account (Jackson et al., 2005). Despite the carbon sequestration advantages of invasive plants over natives, the water demand of invasive plants tends to increase if another of the same characteristics displaces one species. In that case, the influence on carbon capture and water usage will depend highly on particular species traits and climate and may be difficult to predict. As such, species capable of collecting osmolytes will be fitter and have enhanced survival rates in ecosystems where water is a limited element (in both water and salt stress extremes) (Pintó-Marijuan and Munné-Bosch, 2013). These findings point to the potential for invasive species to have phenomenal effects on the hydrology of a catchment and the hydrological cycle of an ecosystem, highlighting the need for a comprehensive understanding of processes at multiple scales and, as a result, for intensive studies incorporating ecology, hydrology, and invasion biology.

4. Conclusion

In this study, *S. alterniflora* exhibited higher average ET rates of 8.16 mm day⁻¹ than *P. australis*, with mean seasonal estimates of about 6.35 mm day⁻¹. The differences in ET found between invasive and native plants can be attributable to photosynthetic cycling and structural traits that have a high connection with Kc, as hypothesized. Both species' Kc temporal patterns mirrored the characteristic trapezoidal shape of Kc for crops, with the former exhibiting higher values than the latter, owing to the abundant water supply. Since its introduction into China in 1979, *S. alterniflora* was declared an invasive species in 2003, and it now occupies over 50,000 ha of predominantly coastal wetlands (Meng et al., 2020), whereas *P. australis*, on the other hand, currently covers ~33,193 ha (Chen et al., 2022). Based on mean ET rates found in this study, *S. alterniflora* invasion accounts for ~4.3 × 10⁶ m³ day⁻¹ of water loss to evaporation compared to ~1.22 × 10⁶ m³ day⁻¹ from *P. australis*, thus posing a severe threat to the availability of water resources in

China's wetlands. While some studies have found that eliminating IAPs improves water resource availability by lowering ET, its primary purpose of preventing coastal wetland erosion by limiting tidal wave energy, retaining sediments, and stimulating vertical accretion remains inevitable.

In addition to (i) discontinuity of vegetation, (ii) deviation of water regime, (iii) soil heterogeneity, and (iv) absence of weighing possibilities, the findings of field investigation were limited by periodic flooding within the wetland marshes, severe shading of the transplanted reeds, and seawater intrusion, particularly in the unreclaimed marshes. However, combining field measurements (in seawall reclaimed marshes) and mathematical models provide better ET estimates. We recommend that further field studies over broader scales and longer seasons be carried out in other world regions, considering that *S. alterniflora* and *P. australis* are reversed in the USA compared to China, for example. Furthermore, when estimating the daily ET of the reed marsh using the FAO 56 technique, daily Kc rather than a single Kc should be employed. The Kc (*S. alterniflora*) value reported in this study was found to be similar to other wetland plants reported, suggesting that wetland engineers could use the data to determine water budgets for large-scale reed bed ecosystem construction projects in China.

Even though the integration of *surface resistance* and *Penman-Monteith* models proved to be a useful method for ET estimation, with RMSEs on par with traditional errors derived from measurements by eddy covariance, the increasing demand for exact ET data at spatio-temporal scales from technologists and policymakers necessitates the expansion of new and existing assessment networks. More approaches, such as the ones provided by Hughes et al. (1998) and Gassmann et al. (2019) that provide for the modification of potential ET based on soil moisture content, may be beneficial to assess the impacts of tides and rainfall on surface resistance. Though *S. alterniflora* spread can be effective in ecosystem restoration over short periods, assessing the advantages of management measures in the context of global climate change mitigation may be more challenging. The ensuing strategies would effectively reduce *S. alterniflora*'s ET water footprint in wetlands. (i) WUE can be improved at the canopy level by adopting measures to minimize sediment-water evaporation (such as mulching) and redirect more water towards transpiration. (ii) considering the tradeoffs between the positive and negative consequences of *S. alterniflora* invasion, wetland stakeholders in charge of water resource management and restoration must define their goals and success criteria before embarking on ecosystem restoration projects involving invasive wetland plants.

Funding

This work was supported by the National Natural Science Foundation of China (32071521, 31800429), the Natural Science Foundation of Jiangsu Province (BK20170540, BK20211321), the MEL Visiting Fellowship of Xiamen University and Jiangsu Collaborative Innovation Center of Technology and Material of Water Treatment, China.

Declaration of Competing Interest

The authors declare that they have no known competing financial interests or personal relationships that could have appeared to influence the work reported in this paper.

Appendix

For the purpose of calculating reference ET_0 , the mean **saturation vapor pressure**, e_s for a day, week, decade, or month can be calculated as the average of the saturation vapor pressure at the mean daily maximum and minimum air temperatures for that period

$$e_s = \frac{0.6108 \exp\left(\frac{17.27T_{\max}}{T_{\max}+237.3}\right) + 0.6108 \exp\left(\frac{17.27T_{\min}}{T_{\min}+237.3}\right)}{2} \quad (\text{A.1})$$

The **actual vapor pressure**, e_a could be calculated from the relative humidity, based on the availability of the humidity data.

$$e_a = \frac{RH}{100} e_s \quad (\text{A.2})$$

Where RH is daily mean **relative humidity** (%).

It is essential to obtain the slope of the relationship between saturation vapor pressure and temperature Δ (Allen et al., 2006).

$$\Delta = \frac{4098 \left[0.6108 \exp \left(\frac{17.27 T_{mean}}{(T_{mean} + 237.3)} \right) \right]}{(T_{mean} + 237.3)^2} \quad (\text{A.3})$$

$$T_{mean} = \frac{T_{max} + T_{min}}{2} \quad (\text{A.4})$$

Where T_{mean} is mean daily air temperature ($^{\circ}\text{C}$); T_{max} is daily maximum air temperature ($^{\circ}\text{C}$); T_{min} is daily minimum air temperature ($^{\circ}\text{C}$). the psychrometric constant, γ , is given by:

$$\gamma = \frac{C_p P}{\varepsilon \lambda} = 0.000665 P \quad (\text{A.5})$$

Where γ is the psychrometric constant ($\text{kPa}/^{\circ}\text{C}$); P is the atmospheric pressure (kPa); C_p is the specific heat at constant pressure ($1013 \text{ J/kg}/^{\circ}\text{C}$); ε is the ratio of molecular weight of water to dry air (0.622); λ is the latent heat of vaporization (2.45 M J/kg).

The **inverse relative distance earth-sun**, d_r and the **solar inclination**, δ are given by

$$d_r = 1 + 0.033 \cos \left(\frac{2\pi}{365} J \right) \quad (\text{A.6})$$

$$\delta = 0.409 \sin \left(\frac{2\pi}{365} J - 1.39 \right) \quad (\text{A.7})$$

Where, J is the number of days in a year between 1 (1 January) and 365 or 366 (31 December).

The **sunset hour angle**, ω_s is given by

$$\omega_s = \arccos(-\tan(\varphi)\tan(\delta)) \quad (\text{A.8})$$

Where, φ is latitude of the site expressed in radians, δ is solar declination.

The **extraterrestrial radiation**, R_a can be calculated using the solar constant, solar declination, and the time of year for each day of the year and for different latitudes:

$$R_a = \frac{24 \times 60}{\pi} G_{SC} d_r [\omega_s \sin(\varphi) \sin(\delta) + \sin(\omega_s) \cos(\varphi) \cos(\delta)] \quad (\text{A.9})$$

Where G_{SC} is solar constant ($0.0820 \text{ MJ/m}^2/\text{min}$); other parameters defined above.

The **clear sky radiation**, R_{so} is obtainable by:

$$R_{so} = (0.75 + 2E10^{-5}Z) R_a \quad (\text{A.10})$$

Z is the elevation above sea level, (m), other parameters have been defined earlier.

The **net shortwave radiation**, R_{ns} generated by a balance of incoming and reflected solar energy (Allen et al., 2006; Valiantzas, 2006) is given as:

$$R_{ns} = (1 - \alpha) R_s \quad (\text{A.11})$$

Where, R_{ns} is the net solar wave radiation, ($\text{MJ/m}^2/\text{day}$); α is the albedo or canopy reflection coefficient, which is 0.20–0.25 for green vegetation cover dimensionless (Allen et al., 1998a, 1998b); R_s is the incoming solar radiation, ($\text{MJ/m}^2/\text{day}$), given as:

$$R_s = \left(a_s + b_s \frac{n}{N} \right) R_a \quad (\text{A.12})$$

Where a_s is the regression constant, which is the fraction of extraterrestrial radiation that reaches the earth during cloudy days ($n = 0$), $a_s + b_s$ is the fraction of extraterrestrial radiation reaching the earth on clear days ($n = N$), a_s and b_s are calculated based on the actual solar radiation data of the Yancheng Meteorological Bureau of Jiangsu Province weather stations.

The maximum possible duration of daylight N (h) is given as:

$$N = \frac{24}{\pi} \omega_s \quad (\text{A.13})$$

The **net radiation**, R_n is the difference between the incoming net shortwave radiation, R_{ns} and the outgoing net longwave radiation, R_{nl} .

$$R_n = R_{ns} - R_{nl} \quad (\text{A.14})$$

R_{nl} is the net outgoing long wave radiation, ($\text{MJ/m}^2/\text{day}$).

The wind function $f_{(w)}$ is given by:

$$f_{(w)} = a + bU_2 \quad (\text{A.15})$$

Where a and b are wind function coefficients; U_2 is wind speed at 5 m height (m/s). $a = 0$ and $b = 0.536$, were utilized to estimate ET in this study (Linacre, 1993).

$$\rho_a = 1.293 \times \frac{P}{101.325} \times \frac{273.15}{T_a + 273.15} \quad (\text{A.16})$$

The decoupling coefficient (Ω) was developed by Jarvis and McNaughton (1986) by transforming the PM equation:

$$\Omega = \frac{\varepsilon + 1}{\varepsilon + 1 + r_s/r_a} \quad (\text{A.17})$$

Where $\varepsilon = M_w/M_d = 0.622$, M_w and M_d are the water and dry air molar mass, respectively. The decoupling coefficient determines how important r_s and R_n are to ET variability.

The 15-min Q_G and T_s data were used to determine the surface soil heat flux:

$$Q_{GO} = C_s \frac{\Delta T_s}{\Delta t} \Delta z + Q_G \quad (\text{A.18})$$

Where ΔT_s is the soil temperature variation for $\Delta t = 15\text{-min}$ at the [0, 0.1 m] soil layer. The soil heat capacity (C_s) relies on soil moisture (ϑ_s) estimated monthly by the gravimetric method. Each month was categorized as wet or dry weather based on whether the soil water content was greater than or less than 60% of the potential soil moisture content (Hillel, 1998) and C_s data from (Oke and Cleugh, 1987). A soil water balance model was used to estimate daily values of ϑ_s (Gassmann et al., 2011).

References

- Acreman, M.C., Harding, R.J., Lloyd, C.R., McNeil, D.D., 2003. Evaporation characteristics of wetlands: experience from a wet grassland and a reedbed using eddy correlation measurements. *Hydrol. Earth Syst. Sci.* 7, 11–21. <https://doi.org/10.5194/hess-7-11-2003>.
- Alfieri, J.G., Niyyogi, D., Blanken, P.D., Chen, F., LeMone, M.A., Mitchell, K.E., Ek, M.B., Kumar, A., 2008. Estimation of the minimum canopy resistance for croplands and grasslands using data from the 2002 international H2O project. *Mon. Weather Rev.* 136, 4452–4469. <https://doi.org/10.1175/2008MWR2524.1>.
- Allen, R.G., Prueger, J.H., Hill, R.W., 1992. Evapotranspiration from isolated stands of hydrophytes. *Cattail and bulrush*. *Trans. Am. Soc. Agric. Eng.* 35, 1191–1198. <https://doi.org/10.13031/2013.28719>.
- Allen, R.G., Pereira, L.S., Raes, D., 1998a. Crop Evapotranspiration-Guidelines for Computing Crop Water Requirements-FAO Irrigation and Drainage Paper 56 Table of Contents. scourt.org.
- Allen, R.G., Pereira, L.S., Raes, D., Smith, M., 1998b. *Crop Evapotranspiration Guidelines for Computing Crop Water Requirements*, FAO Irrigation & Drainage Paper 56. FAO, Food and Agriculture Organization of the United Nations, Roma.
- Allen, R.G., Pereira, L.S., Raes, D., Smith, M., 2006. FAO Irrigation and Drainage Paper - Crop Evapotranspiration - Guidelines for computing crop water requirements. *Remote Sens. Environ.* 300, 333.
- Amer, K., Hatfield, J., 2004. Canopy Resistance as Affected by Soil and Meteorological Factors in Potato. Publ. from USDA-ARS / UNL Fac.
- ASCE. 1996. ASCE Manuals and Reports on Engineering Practice. In: *Hydrology handbook*, 2nd editionVol. No. 28. ASCE, New York.
- Bidlake, W.R., Woodham, W.M., Lopez, M.A., 1996. Evapotranspiration from areas of native vegetation in west-central Florida. In: US Geol Surv Water Supply Pap, 2430, pp. 1–35.
- Borin, M., Milani, M., Salvato, M., Toscano, A., 2011. Evaluation of Phragmites australis (Cav.) Trin. evapotranspiration in Northern and Southern Italy. *Ecol. Eng.* 37, 721–728. <https://doi.org/10.1016/j.ecoleng.2010.05.003>.
- Brauman, K.A., Daily, G.C., Duarte, T.K., Mooney, H.A., 2007. The nature and value of ecosystem services: an overview highlighting hydrologic services. *Annu. Rev. Environ. Resour.* 32, 67–98. <https://doi.org/10.1146/annurev.energy.32.031306.102758>.
- Burba, G.G., Anderson, D.J., Amen, J.L., 2007. Eddy covariance method: overview of general guidelines and conventional workflow. *AGU Fall Meet Abstr* 1, 1575.
- Burgooon, P.S., Kirkbride, K.F., Henderson, M., Landon, E., 1997. Reed beds for biosolids drying in the arid northwestern United States. *Water Sci. Technol.* 35, 287–292. [https://doi.org/10.1016/S0273-1223\(97\)00081-4](https://doi.org/10.1016/S0273-1223(97)00081-4).
- Calder, I., Dye, P., 2001. Hydrological impacts of invasive alien plants. *L Use Water Resour Res* 1, 1–12.
- Catford, J.A., 2017. Hydrological impacts of biological invasions. *Impact Biol Invasions Ecosyst Serv* 12, 63–80. https://doi.org/10.1007/978-3-319-45121-3_5.
- Cavalieri, M.A., Lawren, S., 2010. Comparative water use of native and invasive plants at multiple scales: a global meta-analysis. *Ecology* 91, 2705–2715. <https://doi.org/10.1890/09-0582.1>.
- Chazarenc, F., Merlin, G., Gonthier, Y., 2003. Hydrodynamics of horizontal subsurface flow constructed wetlands. *Ecol. Eng.* 21, 165–173. <https://doi.org/10.1016/j.ecoleng.2003.12.001>.
- Chen, J., 2013. Dynamic geomorphology characteristics research near the tidal flat of the Liangduo River Gate, Jiangsu. In: International Conference on Remote Sensing, Environment and Transportation Engineering, 2013. RSETE, pp. 51–54. <https://doi.org/10.2991/rsete.2013.13>.
- Chen, G., Jin, R., Ye, Z., Li, Q., Gu, J., Luo, M., Luo, Y., Christakos, G., Morris, J., He, J., Li, D., Wang, H., Song, L., Wang, Q., Wu, J., 2022. Spatiotemporal mapping of salt marshes in the intertidal zone of China during 1985–2019. *J. Remote Sens* 1–15. <https://doi.org/10.34133/2022/9793626>.
- Dacey, J.W.H., Howes, B.L., 1984. Water uptake by roots controls water table movement and sediment oxidation in short Spartina marsh. *Science* (80-) 224, 487–489. <https://doi.org/10.1126/science.224.4648.487>.
- Dawson, T.E., Burgess, S.S.O., Tu, K.P., Oliveira, R.S., Santiago, L.S., Fisher, J.B., Simonin, K.A., Ambrose, A.R., 2007. Nighttime transpiration in woody plants from contrasting ecosystems. *Tree Physiol.* 27, 561–575. <https://doi.org/10.1093/TREEPHY/27.4.561>.
- De Gong, H., Geng, Y.J., Yang, C., Jiao, D.Y., Chen, L., Cai, Z.Q., 2018. Yield and resource use efficiency of *Plukenetia volubilis* plants at two distinct growth stages as affected by irrigation and fertilization. *Sci. Rep.* 8, 1–14. <https://doi.org/10.1038/s41598-017-18342-6>.
- Dolman, A.J., Miralles, D.G., De Jeu, R.A.M., 2014. Fifty years since Monteith's 1965 seminal paper: the emergence of global ecohydrology. *Ecohydrology* 7, 897–902. <https://doi.org/10.1002/ECO.1505>.
- Doorenbos, J., Pruitt, W.O., 1984. Crop water requirements. In: *FAO Irrigation and Drainage Paper* 24, 21. FAO, Rome. Rome Food Agric Organ United Nations.
- Drake, J.E., Tjoelker, M.G., Värvhammar, A., Medlyn, B.E., Reich, P.B., Leigh, A., Pfautsch, S., Blackman, C.J., López, R., Aspinwall, M.J., Crous, K.Y., Duursma, R.A., Kumaraanthunge, D., De Kauwe, M.G., Jiang, M., Nicotra, A.B., Tissue, D.T., Choat, B., Atkin, O.K., Barton, C.V.M., 2018. Trees tolerate an extreme heatwave via sustained transpirational cooling and increased leaf thermal tolerance. *Glob. Chang. Biol.* 24, 2390–2402. <https://doi.org/10.1111/gcb.14037>.
- Drexler, J.Z., Snyder, R.L., Spano, D., Paw, U., 2004. A review of models and micrometeorological methods used to estimate wetland evapotranspiration. *Hydrolog. Process.* 18, 2071–2101. <https://doi.org/10.1002/hyp.1462>.
- Dzikiti, S., Steppé, K., Lemeur, R., Milford, J., 2007. Whole-tree level water balance and its implications on stomatal oscillations in orange trees [*Citrus sinensis* (L.) Osbeck] under natural climatic conditions. *J. Exp. Bot.* 58, 1893–1901. <https://doi.org/10.1093/JXB/ERM023>.
- Dzikiti, S., Gush, M.B., Le Maitre, D.C., Maherry, A., Jovanovic, N.Z., Ramoelo, A., Cho, M.A., 2016. Quantifying potential water savings from clearing invasive alien *Eucalyptus camaldulensis* using in situ and high resolution remote sensing data in the Berg River Catchment, Western Cape, South Africa. *For. Ecol. Manag.* 361, 69–80. <https://doi.org/10.1016/J.FORECO.2015.11.009>.
- Eichelmann, E., Hemes, K.S., Knox, S.H., Oikawa, P.Y., Chamberlain, S.D., Sturtevant, C., Verfaillie, J., Baldocchi, D.D., 2018. The effect of land cover type and structure on evapotranspiration from agricultural and wetland sites in the Sacramento-San Joaquin River Delta, California. *Agric. For. Meteorol.* 256–257, 179–195. <https://doi.org/10.1016/J.AGRFORMAT.2018.03.007>.
- El Hamouri, B., Nazih, J., Lahjouj, J., 2007. Subsurface-horizontal flow constructed wetland for sewage treatment under Moroccan climate conditions. *Desalination* 215, 153–158. <https://doi.org/10.1016/j.desal.2006.11.018>.
- Everard, M., 2020. Can management of 'thirsty' alien trees improve water security in semi-arid India? *Sci. Total Environ.* 704, 135451. <https://doi.org/10.1016/J.SCITOVEN.2019.135451>.
- Ewe, S.M.L., Sternberg, L.D.S.L., 2002. Seasonal water-use by the invasive exotic, *Schinus terebinthifolius*, in native and disturbed communities. *Oecologia* 133, 441–448. <https://doi.org/10.1007/s00442-002-1047-9>.
- Fang, S.B., Xu, C., Jia, X.B., Wang, B.Z., An, S.Q., 2010. Using heavy metals to detect the human disturbances spatial scale on Chinese Yellow Sea coasts with an integrated analysis. *J. Hazard. Mater.* 184, 375–385. <https://doi.org/10.1016/J.JHAZMAT.2010.08.046>.
- Farley, K.A., Jobbágy, E.G., Jackson, R.B., 2005. Effects of afforestation on water yield: a global synthesis with implications for policy. *Glob. Chang. Biol.* 11, 1565–1576. <https://doi.org/10.1111/j.1365-2486.2005.01011.X>.
- Fermor, P.M., Hedges, P.D., Gilbert, J.C., Gowing, D.J.G., 2001. Reedbed evapotranspiration rates in England. *Hydrolog. Process.* 15, 621–631. <https://doi.org/10.1002/hyp.174>.
- Funk, J.L., Vitousek, P.M., 2007. Resource-use efficiency and plant invasion in low-resource systems. *Nat* 2007, 1079–1081. <https://doi.org/10.1038/nature05719>, 4467139 446.
- Funk, J.L., Zachary, V.A., 2010. Physiological responses to short-term water and light stress in native and invasive plant species in southern California. *Biol. Invasions* 12, 1685–1694. <https://doi.org/10.1007/s10530-009-9581-6>.
- Gassmann, M., Gardiol, J., Serio, L., 2011. Performance evaluation of evapotranspiration estimations in a model of soil water balance. *Meteorol. Appl.* 18, 211–222. <https://doi.org/10.1002/MET.231>.
- Gassmann, M.I., Toni, N.E., Burek, A., Pérez, C.F., 2019. Estimation of evapotranspiration of a salt marsh in southern South America with coupled Penman-

- Monteith and surface resistance models. Agric. For. Meteorol. 266–267, 109–118. <https://doi.org/10.1016/j.agrformet.2018.12.003>.
- Gavencik, S., 1972. Etude Des Pertes D'eau Par Evapotranspiration Des Plantes Aquatiques [Etude Des Pertes D'eau Par Evapotranspiration Des Plantes Aquatiques].
- Gilman, K., 1993. Hydrology and freshwater wetland conservation. In: Proceedings of MAFF Conference of River and Coastal Engineers. Institute of Hydrology University of Loughborough, Loughborough, UK, pp. 9.2.1–9.2.14.
- Giurgevich, J.R., Dunn, E.L., 1979. Seasonal patterns of CO₂ and water vapor exchange of the tall and short height forms of *Spartina alterniflora* Loisel in a Georgia salt marsh. Oecologia 43, 139–156. <https://doi.org/10.1007/BF00344767>.
- Giurgevich, J.R., Dunn, E.L., 1982. Seasonal patterns of daily net photosynthesis, transpiration and net primary productivity of *Juncus roemerianus* and *Spartina alterniflora* in a Georgia salt marsh. Oecologia 52, 404–410. <https://doi.org/10.1007/BF00367967>.
- Goto, K., Yabuta, S., Ssenyonga, P., Tamaru, S., Sakagami, J.I., 2021. Response of leaf water potential, stomatal conductance and chlorophyll content under different levels of soil water, air vapor pressure deficit and solar radiation in chili pepper (*Capsicum chinense*). Sci Hortic Amsterdam 281, 109943. <https://doi.org/10.1016/j.scienta.2021.109943>.
- Grotkopp, E., Rejmánek, M., Rost, T.L., 2002. Toward a causal explanation of plant invasiveness: Seedling growth and life-history strategies of 29 pine (*Pinus*) species. Am. Nat. 159, 396–419. <https://doi.org/10.1086/338995>.
- Hassan, S., Shariff, A.R.M., Amin, M.S.M., 2008. A comparative study of evapotranspiration calculated from remote sensing, meteorological and lysimeter data. In: 3rd International Conference on Water Resources and Arid Environments, p. 11.
- Headley, T.R., Davison, L., Huett, D.O., Müller, R., 2012. Evapotranspiration from subsurface horizontal flow wetlands planted with *Phragmites australis* in subtropical Australia. Water Res. 46, 345–354. <https://doi.org/10.1016/j.watres.2011.10.042>.
- Herbst, M., Kappen, L., 1999. The ratio of transpiration versus evaporation in a reed belt as influenced by weather conditions. Aquat. Bot. 63, 113–125. [https://doi.org/10.1016/S0304-3770\(98\)00112-0](https://doi.org/10.1016/S0304-3770(98)00112-0).
- Hester, M.W., Mendelsohn, I.A., McKee, K.L., 2001. Species and population variation to salinity stress in *Panicum hemitomon*, *Spartina patens*, and *Spartina alterniflora*: Morphological and physiological constraints. In: Environmental and Experimental Botany. Elsevier, pp. 277–297. [https://doi.org/10.1016/S0098-8472\(01\)00100-9](https://doi.org/10.1016/S0098-8472(01)00100-9).
- Hillel, Daniel, 1998. Environmental soil physics: fundamentals, applications, and environmental considerations. Environ. Soil Phys. 1st Edition, 1–800.
- Hölttä, T., Dominguez Carrasco, M.D.R., Salmon, Y., Aalto, J., Vanhatalo, A., Bäck, J., Lintunen, A., 2018. Water relations in silver birch during springtime: how is sap pressurised? Plant Biol. 20, 834–847. <https://doi.org/10.1111/plb.12838>.
- Howes, B.L., Dacey, J.W.H., Goehringer, D.D., 1986. Factors controlling the growth form of *spartina alterniflora*: feedbacks between above-ground production, sediment oxidation, nitrogen and salinity. J. Ecol. 74, 881. <https://doi.org/10.2307/2260404>.
- Hughes, C.E., Binning, P., Willgoose, G.R., 1998. Characterisation of the hydrology of an estuarine wetland. J. Hydrol. 211, 34–49. [https://doi.org/10.1016/S0022-1694\(98\)00194-2](https://doi.org/10.1016/S0022-1694(98)00194-2).
- Hughes, A.L.H., Wilson, A.M., Morris, J.T., 2012. Hydrologic variability in a salt marsh: Assessing the links between drought and acute marsh dieback. Estuar. Coast. Shelf Sci. 111, 95–106. <https://doi.org/10.1016/j.ecss.2012.06.016>.
- Hussey, B.H., Odum, W.E., 1992. Evapotranspiration in tidal marshes. Estuaries 15, 59–67. <https://doi.org/10.2307/1352710>.
- Huxman, T.E., Wilcox, B.P., Breshears, D.D., Scott, R.L., Snyder, K.A., Small, E.E., Hultine, K., Pockman, W.T., Jackson, R.B., 2005. Ecohydrological implications of woody plant encroachment. Ecology 86, 308–319. <https://doi.org/10.1890/03-0583>.
- Irvine, J., Law, B.E., Kurpius, M.R., Anthoni, P.M., Moore, D., Schwarz, P.A., 2004. Age-related changes in ecosystem structure and function and effects on water and carbon exchange in ponderosa pine. Tree Physiol. 24, 753–763. <https://doi.org/10.1093/treephys/24.7.753>.
- Jackson, R.B., Jobbagy, E.G., Avissar, R., Roy, S.B., Barrett, D.J., Cook, C.W., Farley, K.A., Le Maitre, D.C., McCarl, B.A., Murray, B.C., 2005. Atmospheric science: trading water for carbon with biological carbon sequestration. Science (80.-) 310, 1944–1947. <https://doi.org/10.1126/SCIENCE.1119282>.
- Jarvis, P.G., McNaughton, K.G., 1986. Stomatal control of transpiration: scaling up from leaf to region. Adv. Ecol. Res. 15, 1–49. [https://doi.org/10.1016/S0065-2504\(08\)60119-1](https://doi.org/10.1016/S0065-2504(08)60119-1).
- Jiang, L.F., Luo, Y.Q., Chen, J.K., Li, B., 2009. Ecophysiological characteristics of invasive *Spartina alterniflora* and native species in salt marshes of Yangtze River estuary, China. Estuar. Coast. Shelf Sci. 81, 74–82. <https://doi.org/10.1016/j.ecss.2008.09.018>.
- Kagawa, A., Sack, L., Duarte, K., James, S., 2009. Hawaiian native forest conserves water relative to timber plantation: Species and stand traits influence water use. Ecol. Appl. 19, 1429–1443. <https://doi.org/10.1890/08-1704.1>.
- Królikowska, J., 1971. Transpiration of reed (*Phragmites communis* Trin.). Polish Archives of Hydrobiology 18 (4), 347–358.
- Le Maître, D.C., Scott, D.F., Colvin, C., 1999. A review of information on interactions between vegetation and groundwater. Water SA 25, 137–152.
- Le Maître, D.C., Blignaut, J.N., Clulow, A., Dzikiti, S., Everson, C.S., Görgens, A.H.M., Gush, M.B., 2020. Impacts of plant invasions on terrestrial water flows in South Africa. In: Biological Invasions in South Africa. Springer International Publishing, pp. 431–457. https://doi.org/10.1007/978-3-030-32394-3_15.
- Leishman, M.R., Haslehurst, T., Ares, A., Baruch, Z., 2007. Leaf trait relationships of native and invasive plants: Community- and global-scale comparisons. New Phytol. 176, 635–643. <https://doi.org/10.1111/j.1469-8137.2007.02189.x>.
- Leuning, R., Zhang, Y.Q., Rajaud, A., Cleugh, H., Tu, K., 2008. A simple surface conductance model to estimate regional evaporation using MODIS leaf area index and the Penman-Monteith equation. Water Resour. Res. 44, 10419. <https://doi.org/10.1029/2007WR006562>.
- Linacre, E.T., 1993. Data-sparse estimation of lake evaporation, using a simplified Penman equation. Agric. For. Meteorol. 64, 237–256. [https://doi.org/10.1016/0168-1923\(93\)90031-C](https://doi.org/10.1016/0168-1923(93)90031-C).
- Linthurst, R.A., Seneca, E.D., 1980. The effects of standing water and drainage potential on the *Spartina Alterniflora*-substrate complex in a North Carolina salt marsh. Estuar. Coast. Mar. Sci. 11, 41–52. [https://doi.org/10.1016/S0302-3524\(80\)80028-4](https://doi.org/10.1016/S0302-3524(80)80028-4).
- Ma, Y.J., Li, X.Y., Wilson, M., Wu, X.C., Smith, A., Wu, J., 2016. Water loss by evaporation from China's South-North Water transfer Project. Ecol. Eng. 95, 206–215. <https://doi.org/10.1016/j.ecoleng.2016.06.086>.
- Mariotti, G., Kearney, W.S., Fagherazzi, S., 2019. Soil creep in a mesotidal salt marsh channel bank: Fast, seasonal, and water table mediated. Geomorphology 334, 126–137. <https://doi.org/10.1016/j.geomorph.2019.03.001>.
- Mathias, J.M., Thomas, R.B., 2021. Global tree intrinsic water use efficiency is enhanced by increased atmospheric CO₂ and modulated by climate and plant functional types. Proc. Natl. Acad. Sci. U. S. A. 118, 2014286118, 10.1073/PNAS.2014286118/-DCSUPPLEMENTAL.
- McCormick, F.H., Contreras, G.C., 2009. Effects of nonindigenous invasive species on water quality and quantity. A Dyn Invasive SpeciesRes Vis Oppor Priorities 111–120.
- McDowell, S.C.L., 2002. Photosynthetic characteristics of invasive and noninvasive species of Rubus (Rosaceae). Am. J. Bot. 89, 1431–1438. <https://doi.org/10.3732/ajb.89.9.1431>.
- McNaughton, K., Jarvis, P.G., 1983. Predicting effects of vegetation changes on transpiration and evaporation. In: Additional Woody Crop Plants, pp. 1–47. <https://doi.org/10.1016/B978-0-12-424157-2.50007-0>.
- Meijninger, W.M.L., Jarman, C., 2014. Satellite-based annual evaporation estimates of invasive alien plant species and native vegetation in South Africa. Water SA 40, 95–107. <https://doi.org/10.4314/wsa.v40i1.12>.
- Mendelsohn, I.A., Seneca, E.D., 1980. The influence of soil drainage on the growth of salt marsh cordgrass *Spartina alterniflora* in North Carolina. Estuar. Coast. Mar. Sci. 11, 27–40. [https://doi.org/10.1016/S0302-3524\(80\)80027-2](https://doi.org/10.1016/S0302-3524(80)80027-2).
- Meng, W., Feagin, R.A., Innocenti, R.A., Hu, B., He, M., Li, H., 2020. Invasion and ecological effects of exotic smooth cordgrass *Spartina alterniflora* in China. Ecol. Eng. 143, 105670 <https://doi.org/10.1016/J.ECOLENG.2019.105670>.
- Milani, M., Toscano, A., 2013. Evapotranspiration from pilot-scale constructed wetlands planted with *Phragmites australis* in a Mediterranean environment. J. Environ. Sci. Heal. - Part A Toxic/Hazardous Subst Environ Eng 48, 568–580. <https://doi.org/10.1080/10934529.2013.730457>.
- Milani, M., Marzo, A., Toscano, A., Consoli, S., Cirelli, G.L., Ventura, D., Barbagallo, S., 2019. Evapotranspiration from Horizontal Subsurface Flow Constructed Wetlands Planted With Different Perennial Plant Species. mdpi.com. <https://doi.org/10.3390/w11102159>.
- Monteith, J., Unsworth, M., 2007. Principles of Environmental Physics, 3rd edition. NY, USA, New York.
- Oke, T.R., Cleugh, H.A., 1987. Urban heat storage derived as energy balance residuals. Boundary-Layer Meteorol 393 (39), 233–245. <https://doi.org/10.1007/BF00116120>.
- Pauliukonis, N., Schneider, R., 2001. Temporal patterns in evapotranspiration from lysimeters with three common wetland plant species in the eastern United States. Aquat. Bot. 71, 35–46. [https://doi.org/10.1016/S0304-3770\(01\)00168-1](https://doi.org/10.1016/S0304-3770(01)00168-1).
- Peacock, C.E., Hess, T.M., 2004. Estimating evapotranspiration from a reed bed using the Bowen ratio energy balance method. Hydrol. Process. 18, 247–260. <https://doi.org/10.1002/hyp.1373>.
- Pintó-Marijuan, M., Munné-Bosch, S., 2013. Ecophysiology of invasive plants: osmotic adjustment and antioxidants. Trends Plant Sci. 18, 660–666. <https://doi.org/10.1016/J.TPLANTS.2013.08.006>.
- Prieto, I., Querejeta, J.I., Segrestin, J., Volaire, F., Roumet, C., 2018. Leaf carbon and oxygen isotopes are coordinated with the leaf economics spectrum in Mediterranean rangeland species. Funct. Ecol. 32, 612–625. <https://doi.org/10.1111/1365-2435.13025>.
- Racelis, A., Wagle, P., Escamilla, J., Goolsby, J., Gowda, P., 2021. Interannual variability and seasonal dynamics of evapotranspiration of *Arundo donax* L. and populations of its biological Control Agent (*Tetramesa romana*). Ecohydrol. Hydrobiol. <https://doi.org/10.1016/J.ECOHYD.2021.07.002>.
- Read, K.E., Hedges, P.D., Fermor, P.M., 2008. Monthly evapotranspiration coefficients of large reed bed habitats in the United Kingdom. Wastewater Treat Plant Dyn Manag Constr Nat Wetl 1, 99–109. https://doi.org/10.1007/978-1-4020-8235-1_9.
- Reich, P.B., Walters, M.B., Tabone, T.J., 1989. Response of *Ulmus americana* seedlings to varying nitrogen and water status. 2 water and nitrogen use efficiency in photosynthesis. Tree Physiol. 5, 173–184. <https://doi.org/10.1093/treephys/5.2.173>.
- Rozkošný, M., Šálek, J., 2006. Water balance of the constructed wetlands—a study of the macrophytes evapotranspiration researchgate.net.
- Schilling, K.E., Kiniry, J.R., 2007. Estimation of evapotranspiration by reed canarygrass using field observations and model simulations. J. Hydrol. 337, 356–363. <https://doi.org/10.1016/j.jhydrol.2007.02.003>.
- Seibt, Ulli, Rajabi, Abazar, Griffiths, Howard, Berry A., Joseph, 2008. Carbon isotopes and water use efficiency: sense and sensitivity. Oecologia 155, 441. <https://doi.org/10.1007/s00442-007-0932-7>.
- Si, J.H., Feng, Q., Zhang, X.Y., Liu, W., Su, Y.H., Zhang, Y.W., 2005. Growing season evapotranspiration from *Tamarix ramosissima* stands under extreme arid conditions

- in Northwest China. *Environ. Geol.* 48, 861–870. <https://doi.org/10.1007/s00254-005-0025-z>.
- Smid, P., 1975. Evaporation from a Reedswamp. *J. Ecol.* 63, 299. <https://doi.org/10.2307/2258856>.
- Snyder, R.L., Boyd, C.E., 1987. Evapotranspiration by *Eichhornia crassipes* (Mart.) Solms and *Typha latifolia* L. *Aquat. Bot.* 27, 217–227. [https://doi.org/10.1016/0304-3770\(87\)90042-8](https://doi.org/10.1016/0304-3770(87)90042-8).
- Souch, C., Wolfe, C.P., Grimmond, C.S.B., 1996. Wetland evaporation and energy partitioning: Indiana Dunes National Lakeshore. *J. Hydrol.* 184, 189–208. [https://doi.org/10.1016/0022-1694\(95\)02989-3](https://doi.org/10.1016/0022-1694(95)02989-3).
- Souch, C., Grimmond, C.S.B., Wolfe, C.P., 1998. Evapotranspiration rates from wetlands with different disturbance histories: Indiana Dunes National Lakeshore. *Wetlands* 18, 216–229. <https://doi.org/10.1007/bf03161657>.
- Swaffer, B.A., Holland, K.L., 2015. Comparing ecophysiological traits and evapotranspiration of an invasive exotic, *Pinus halepensis* in native woodland overlying a karst aquifer. *Ecohydrology* 8, 230–242. <https://doi.org/10.1002/ECO.1502>.
- Tang, L., Mo, K., Chen, Q., Zhang, J., Xia, J., Lin, Y., 2020. An experimental study on potential changes in plant community evapotranspiration due to the invasion of *Hydrocotyle vulgaris*. *J. Hydro-Environment Res* 30, 63–70. <https://doi.org/10.1016/J.JHER.2020.01.003>.
- Tonti, N., Gassmann, M., Covi, M., Pérez, C., Righetti, S., 2020. Balance de Energía Sobre Un Cultivo De Soja. <https://doi.org/10.5902/2179-460X1648>.
- Tordini, E., Petruzzellis, F., Nardini, A., Savi, T., Bacaro, G., 2019. Make it simpler: Alien species decrease functional diversity of coastal plant communities. *J. Veg. Sci.* 30, 498–509. <https://doi.org/10.1111/JVS.12734>.
- Twine, T.E., Kustas, W.P., Norman, J.M., Cook, D.R., Houser, P.R., Meyers, T.P., Prueger, J.H., Starks, P.J., Wesely, M.L., 2000. Correcting eddy-covariance flux underestimates over a grassland. *Agric. For. Meteorol.* 103, 279–300. [https://doi.org/10.1016/S0168-1923\(00\)00123-4](https://doi.org/10.1016/S0168-1923(00)00123-4).
- Unland, H.E., Houser, P.R., Shuttleworth, W.J., Yang, Z.L., 1996. Surface flux measurement and modeling at a semi-arid Sonoran Desert site. *Agric. For. Meteorol.* 82, 119–153. [https://doi.org/10.1016/0168-1923\(96\)02330-1](https://doi.org/10.1016/0168-1923(96)02330-1).
- Valiantzas, J.D., 2006. Simplified versions for the Penman evaporation equation using routine weather data. *J. Hydrol.* 331, 690–702. <https://doi.org/10.1016/j.jhydrol.2006.06.012>.
- Van den Boogaard, R., Villar, R., 1998. Variation in growth and water-use efficiency - a comparison of *Aegilops* L. species and *Triticum aestivum* L. cultivars. In: *Inherent Variation in Plant Growth - Physiological Mechanisms and Ecological Consequences*, pp. 289–308.
- Wang, Q., Wang, C.H., Zhao, B., Ma, Z.J., Luo, Y.Q., Chen, J.K., Li, B., 2006. Effects of growing conditions on the growth of and interactions between salt marsh plants: Implications for invasibility of habitats. *Biol. Invasions* 8, 1547–1560. <https://doi.org/10.1007/s10530-005-5846-x>.
- Watts, D.A., Moore, G.W., 2011. Water-use dynamics of an invasive reed, *Arundo donax*, from leaf to stand. *Wetlands* 31, 725–734. <https://doi.org/10.1007/s13157-011-0188-1>.
- Wessel, D.A., Rouse, W.R., 1994. Modelling evaporation from wetland tundra. *Boundary-Layer Meteorol* 68, 109–130. <https://doi.org/10.1007/BF00712666>.
- Wilks, D.S., 2011. Principal Component (EOF) Analysis, International Geophysics. Academic Press. <https://doi.org/10.1016/B978-0-12-385022-5.00012-9>.
- Wullschleger, S.D., Meinzer, F.C., Vertessey, R.A., 1998. A review of whole-plant water use studies in trees. In: *Tree Physiology*. Oxford University Press, pp. 499–512. <https://doi.org/10.1093/treephys/18.8-9.499>.
- Xiao, J., Sun, G., Chen, J., Chen, H., Chen, S., Dong, G., Gao, S., Guo, H., Guo, J., Han, S., Kato, T., Li, Y., Lin, G., Lu, W., Ma, M., McNulty, S., Shao, C., Wang, X., Xie, X., Zhang, X., Zhang, Z., Zhao, B., Zhou, G., Zhou, J., 2013. Carbon fluxes, evapotranspiration, and water use efficiency of terrestrial ecosystems in China. *Agric. For. Meteorol.* 182–183, 76–90. <https://doi.org/10.1016/j.agrformet.2013.08.007>.
- Yan, C., Zhao, W., Wang, Y., Yang, Q., Zhang, Q., Qiu, G.Y., 2017. Effects of forest evapotranspiration on soil water budget and energy flux partitioning in a subalpine valley of China. *Agric. For. Meteorol.* 246, 207–217. <https://doi.org/10.1016/j.agrformet.2017.07.002>.
- Yu, W.Y., Zhou, G.S., Chi, D.C., Zhou, L., He, Q.J., 2008a. Evapotranspiration of *Phragmites communis* community in Panjin Wetland and its controlling factors. *Shengtai Xuebao. Acta Ecol. Sin.* 28, 4594–4601. [https://doi.org/10.1016/s1872-2032\(08\)60081-5](https://doi.org/10.1016/s1872-2032(08)60081-5).
- Yu, W.Y., Zhou, G.S., Chi, D.C., Zhou, L., He, Q.J., 2008b. Evapotranspiration of *Phragmites communis* community in Panjin wetland and its control factors. *Acta Ecol. Sin.* 28, 4594–4601. [https://doi.org/10.1016/S1872-2032\(08\)60081-5](https://doi.org/10.1016/S1872-2032(08)60081-5).
- Yuguda, T.K., Li, Y., Zhang, W., Ye, Q., 2020. Incorporating water loss from water storage and conveyance into blue water footprint of irrigated sugarcane: a case study of Savannah Sugar Irrigation District, Nigeria. *Sci. Total Environ.* 715 <https://doi.org/10.1016/j.scitotenv.2020.136886>.
- Zeballos, S.R., Giorgis, M.A., Cingolani, A.M., Cabido, M., Whitworth-Hulse, J.I., Gurvich, D.E., 2014. Do alien and native tree species from Central Argentina differ in their water transport strategy? *Austral Ecol* 39, 984–991. <https://doi.org/10.1111/aec.12171>.
- Zhang, J., Sheng, L., Zhang, J., Zhang, S., Zhang, W., Liu, B., Gong, C., Jiang, M., Lv, X., Zhang, J., 2018. Partitioning daily evapotranspiration from a marsh wetland using stable isotopes in a semiarid region. *Hydrol. Res.* 49, 1005–1015. <https://doi.org/10.2166/nh.2017.005>.
- Zhao, C., Nan, Z., Cheng, G., 2005. Methods for estimating irrigation needs of spring wheat in the middle Heihe basin, China. *Agric. Water Manag.* 75, 54–70. <https://doi.org/10.1016/j.agwat.2004.12.003>.
- Zhao, Y., Yang, Z., Xia, X., Wang, F., 2012. A shallow lake remediation regime with *Phragmites australis*: Incorporating nutrient removal and water evapotranspiration. *Water Res.* 46, 5635–5644. <https://doi.org/10.1016/j.watres.2012.07.053>.
- Zhou, L., Zhou, G., 2009. Measurement and modelling of evapotranspiration over a reed (*Phragmites australis*) marsh in Northeast China. *J. Hydrol.* 372, 41–47. <https://doi.org/10.1016/j.jhydrol.2009.03.033>.
- Zhou, L., Zhou, G., Liu, S., Sui, X., 2010. Seasonal contribution and interannual variation of evapotranspiration over a reed marsh (*Phragmites australis*) in Northeast China from 3-year eddy covariance data. *Hydrol. Process.* 24, 1039–1047. <https://doi.org/10.1002/hyp.7545>.